ADVANCES IN INORGANIC CHEMISTRY AND RADIOCHEMISTRY, VOL. 29

# ORGANIC SUPERCONDUCTORS: SYNTHESIS, STRUCTURE, CONDUCTIVITY, AND MAGNETIC PROPERTIES

JACK M. WILLIAMS* AND KIM CARNEIRO**

*Chemistry and Materials Science and Technology Divisions, Argonne National Laboratory Argonne, Illinois, and
**Physics Laboratory I, University of Copenhagen, H. C. Ørsted Institute, Copenhagen, Denmark



## I. Introduction

It is now well established that synthetic materials may be prepared with mechanical properties closely resembling those of elemental metals and alloys. As a result, we have come a long way from the ebonite handles and fragile plastic toys of 30 years ago to the overwhelming occurrence of plastics in modern mechanical structures. Similarly, it is now possible to mimic the electrical properties of elemental metals



Copyright © 1985, by Academic Press, Inc.
All rights of reproduction in any form reserved.

using synthetic materials although the applications of these systems are still at their infancy. Hence, by a synthetic metal we define a compound with electrical properties resembling those of ordinary metals, despite the fact that it contains no metallic elements. And, from a basic scientific point of view, the success in reproducing electrical properties in synthetic metals, including superconductivity, by *designing* appropriate molecular materials is as pronounced as it has been for the mechanical properties.

The first indication that molecular compounds could exhibit interesting electrical properties apart from those of an insulator was given in 1954, when Akamatu *et al.* (*1*) reported a resistivity of $\rho = 10\ \Omega$ cm for a bromine salt of perylene. Normally perylene crystals themselves are insulating with $\rho = 10^{14}$–$10^{16}\ \Omega$ cm; therefore, a dramatic change in electronic structure had occurred. The perylene molecule is shown in Fig. 1.

It was not until 1960 when the molecule TCNQ (tetracyanoquinodimethane, also shown in Fig. 1) was shown to form highly conducting crystals that molecular conductors became the subject of large-scale solid-state investigations (*2*). In particular, $M(TCNQ)_2$ salts, where M is a monovalent cation (alkali metal or organic), have been extensively studied. As is the case for the original bromine–perylene compound, they are semiconductors (i.e., having thermally activated electrical conduction) with activation energies of 50–200 meV, but possibly exhibiting metallic behavior (non thermally activated conduction) at high temperatures. Figure 2, which shows the development of the temperature-dependent resistivity in molecular conductors in a historical perspective, includes $TEA(TCNQ)_2$ (TEA = triethyl ammonium).

During the same period, the understanding of superconductivity in elemental metals underwent dramatic improvements with the development of the now well-known theory of Bardeen, Cooper, and Schrieffer (BCS) (*3*). According to this theory, electrons form bound pairs (the Cooper pairs) as a result of their interactions with the lattice vibrations (the phonons). The upper limit for the superconducting transition temperature is determined by the maximum phonon frequency, the Debye frequency. This understanding led Little (*4*) to propose that high transition temperatures could be achieved in *molecular* metals (if these could be made) since the high frequencies of their internal vibrations might serve to play the same role phonons play in ordinary superconductors. Little's proposal sparked considerable interest and marked the onset of the search for superconductivity in molecular materials. The promise of possible high-temperature superconductivity has remained a goal since that time.

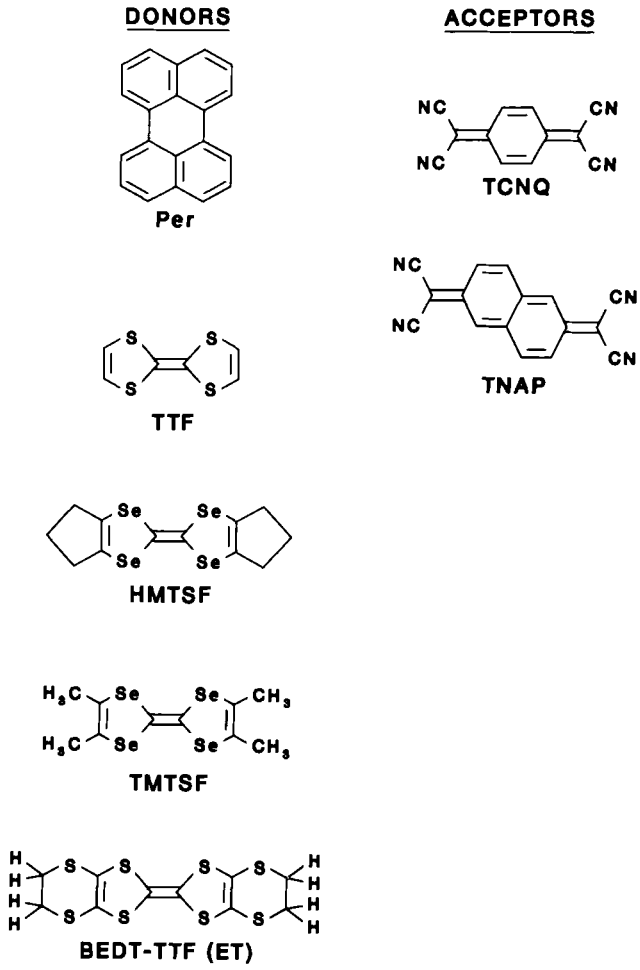


FIG. 1. Molecules that form conducting crystals described in this article. The left column contains the donors: perylene (Per), tetrathiafulvalene (TTF), hexamethylenetetraselenafulvalene (HMTSF), tetramethyltetraselenafulvane (TMTSF), and bis(ethylenedithio)-TTF (BEDT-TTF or "ET"). To the right are the acceptor molecules tetracyanoquinodimethane (TCNQ) and tetracyanonaphthalene (TNAP).

The first molecular crystal exhibiting genuine metallic behavior was TTF-TCNQ (TTF = tetrathiafulvalene) (*5*). Between 54 K and room temperature, TTF-TCNQ behaves like a metal (decreasing electrical resistance with decreasing temperature), although the concept of a metal must of course be modified to take into account the complicated

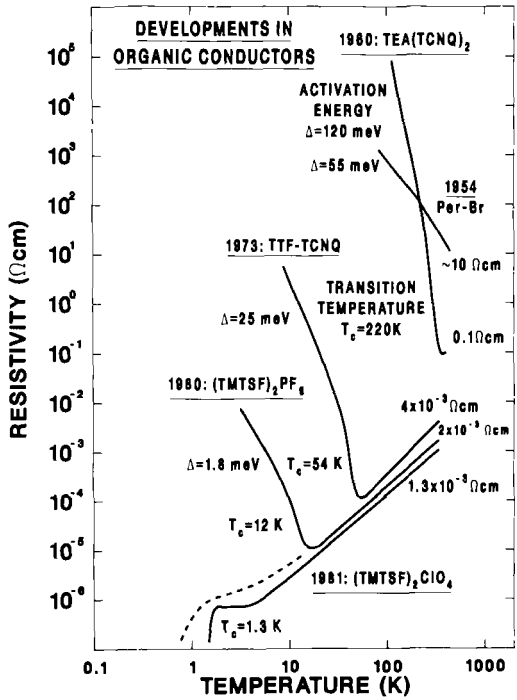


FIG. 2. Temperature dependence of the electrical resistivity of some organic conductors: historical development. The dashed line shows $(TMTSF)_2PF_6$ at high pressure.

electronic structure of a two-component molecular compound. Below 54 K, TTF-TCNQ exists in a semiconducting state similar to the compounds mentioned earlier. This state, often referred to as the Peierls insulator, was predicted to exist in one-dimensional conductors by Peierls in 1954 and arises from an electron–phonon instability of a one-dimensional metal (*6*). The Peierls instability is a clear competitor to superconductivity in molecular conductors since these materials are generally formed by (one-dimensional) stacks of planar, or nearly planar, molecules and these systems tend to undergo lattice distortions, dimerization, etc. at the Peierls transition temperature. Hence, the Peierls instability (and other one-dimensional instabilities to which we shall return) must be prevented by some means if superconductivity is to occur in molecular systems. We now turn to a discussion of the means whereby such transitions, which often result in electron localization, can be suppressed.

One way to induce superconductivity in a molecular metal has proven to be the application of pressure which often prevents or removes the

tendency toward a Peierls transition. Two chemical modifications of the TTF molecule, TMTSF (*7*) (tetramethyltetraselenafulvalene) and BEDT-TTF [bis(ethylenedithio)tetrathiafulvalene] (*8, 9*) form superconductors under pressure and, in a very few cases, at ambient pressure. Several $(TMTSF)_2X$ salts, known as Bechgaard salts ($X = PF_6^-$, $AsF_6^-$, $TaF_6^-$, $FSO_3^-$, and $ReO_4^-$), show this behavior, and in one instance ($X = ClO_4^-$) superconductivity is observed without the application of pressure (*10, 11*). The superconducting transition temperatures ($T_c$) for $(TMTSF)_2X$ and $(BEDT\text{-}TTF)_2X$ materials (X = monovalent anion) range from ~0.9–1.2 K for the former and 1.5–2.7 K for the latter synthetic metals. A number of salts of the BEDT-TTF, or "ET",[1] family exhibit ambient-pressure superconductivity, viz. $\beta$-$(ET)_2I_3$ (*9, 105, 106, 114*) and $\beta$-$(ET)_2IBr_2$ (*107, 108*), while $(ET)_2ReO_4$ requires pressures above 4–6 kbar to suppress a metal–insulator transition that occurs at ~81 K (*8*).

An attempt to explain the physical properties of molecular metals by using the concepts commonly invoked for ordinary metals may seem a very ambitious and highly risky task, and we do not pretend to present here, in any way, the final answers. Nevertheless, we find that penetrating and useful insight is gained by analyzing the crystallographic structures of synthetic metals and correlating them with their solid-state properties as exemplified by their electrical conductivities and magnetic susceptibilities. We shall focus only on TMTSF and ET salts, since they form the basis for all known organic superconductors, and because they display, more or less, all of the structural features and properties of earlier synthetic conductors. And as we will demonstrate, despite the complexity of the problem, it is possible to give several ingredients that contribute to the recipe for the synthesis of an improved synthetic metal or superconductor.

## II. The Synthesis of TMTSF and BEDT-TTF (ET), and Crystal Growth of Conducting Salts

Synthesizing a molecular conductor generally falls into two separate parts. First, the starting material, the organic donor "conducting molecule" has to be prepared, and secondly, single crystals of the desired conducting salts must be grown. Both procedures must be

[1] As it appears from Fig. 1, the short names for "conducting molecules" are descriptive but in no way unambiguous. As even descriptive short names become longer and longer, there may be a need for shortening them. Hence, BEDT-TTF is often abbreviated ET, not entirely independent of the fact that the Spielberg movie "ET" (Extra Terrestrial)® occurred within a few months of the discovery of superconductivity in $(ET)_2ReO_4$ (in a California laboratory).

independently optimized, and, in particular, care must be taken to design the crystal growth procedure in order to maximize the yield of crystals of desired stoichiometry and crystal structure. The latter problem has recently proven to be a severe one for $(ET)_2X$ conductors, which often form a multiplicity of phases, sometimes even of the *same stoichiometry* but with different crystal structures and electrical properties, all during a single growth cycle.

### A. The Synthesis of TMTSF and Chalcogenide Derivatives

The original synthesis of TMTSF required $CSe_2$ as a starting material (*13–15*) and that route has been patented (*16*). Since $CSe_2$ is difficult to handle and extremely malodorous (rotten radishes!), syntheses in which gaseous $H_2Se$ replaced $CSe_2$ in the syntheses of TMTSF were subsequently reported using selenoureas (*17*) or *N,N*-dimethylphosgeneiminium chloride (*18, 19*). A synthesis based on the use of $H_2Se$, and which can easily be accomplished by students, has become available (*20*). However, gaseous $H_2Se$ is extremely toxic, with an approximate $LC_{50}$ (30 min) in guinea pigs of 6 ppm, and must be handled with great care (*21*). Therefore, it is not surprising that a TMTSF synthesis has been developed that does not require either $CSe_2$ or $H_2Se$, but rather uses elemental Se as shown in Scheme 1 (*22*).

Although these improvements in the synthesis of TMTSF were welcome, it appears that the presence of a minor sulfur (<1–2%) impurity is observed in any of the procedures, other than that using $CSe_2$, in which *N,N*-dimethylphosgeneiminium chloride is used as an intermediate. This sulfur impurity apparently suppresses the superconducting transition temperatures of $(TMTSF)_2X$ derivatives; when $X = ClO_4^-$, $T_c$ is reduced by ~0.1–0.3 K from 1.3 K. Careful vacuum gradient sublimation of the *N,N*-dimethylphosgeneiminium chloride apparently results in the removal of the sulfur contaminant (*23*). In passing, it should be noted that the preparation of perdeuterio-TMTSF (*19*), tetraselenafulvalene-TCNQ (*24*), and dibenzotetraselenafulvalene charge-transfer salts have also been reported (*25, 26*).

### B. The Synthesis of BEDT-TTF (ET) and Chalcogenide Derivatives

Sulfur-based ET and alkyl derivatives were prepared (*27, 29*) in the late 1970s using $CS_2$ as starting material. A preparative procedure suitable for student use which involves the reduction of $CS_2$ with metallic sodium has also been developed (*28*), as indicated in Scheme 2.

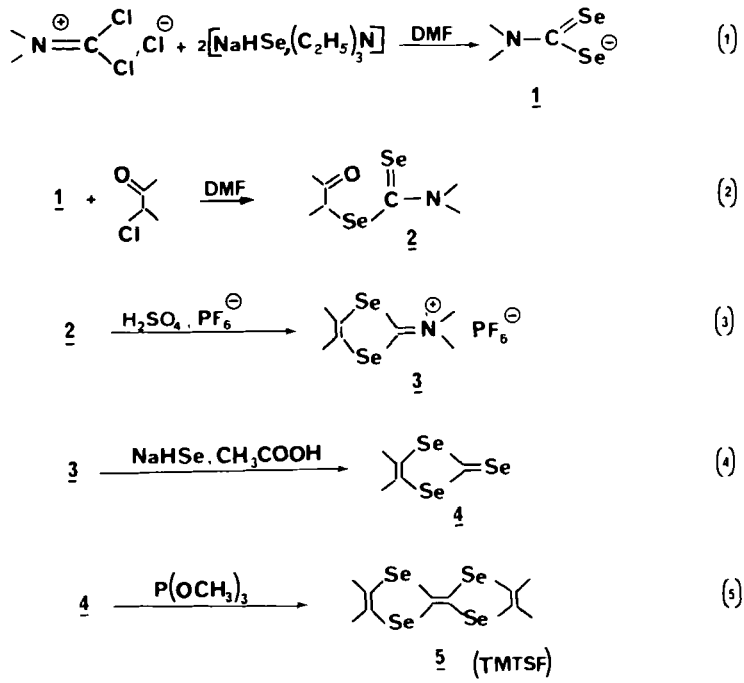

SCHEME 1. Synthesis of TMTSF using elemental selenium (*22*).

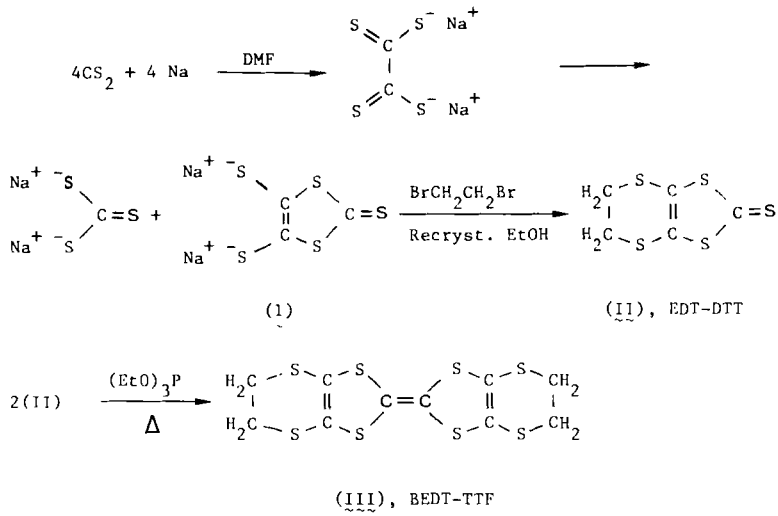

SCHEME 2. Synthesis of BEDT-TTF by reduction of $CS_2$ with metallic sodium (*28*).

Preparative schemes for the systematic modification of the ET framework through the insertion of Se, and S–Se combinations, have been advanced and some derivatives have been prepared (*30*). At this time the only derivatives of ET that form superconductors are for $X = I_3^-$ (*9, 105, 106, 114*), $IBr_2^-$ (*107, 108*), and $ReO_4^-$ (*8*).

## C. Electrocrystallization of 2:1 Derivatives of TMTSF

As mentioned, only 2:1 (radical-cation: monovalent anion) derivatives of organic synmetals appear to form salts that exhibit superconductivity. Crystals of these conductors are produced using simple electrochemical oxidation techniques in an H-shaped cell, or a variation of this type cell, as shown in Fig. 3. Solutions of the organic donor (TMTSF or ET), and a salt of the desired anion as a tetraalkylammonium derivative to increase solubility in the organic medium, are prepared using redistilled, dried, and deoxygenated organic solvents such as tetrahydrofuran or 1,2,2-trichloroethane. Tetrabutylammonium($n$-$Bu_4N^+$) salts are the most commonly used because

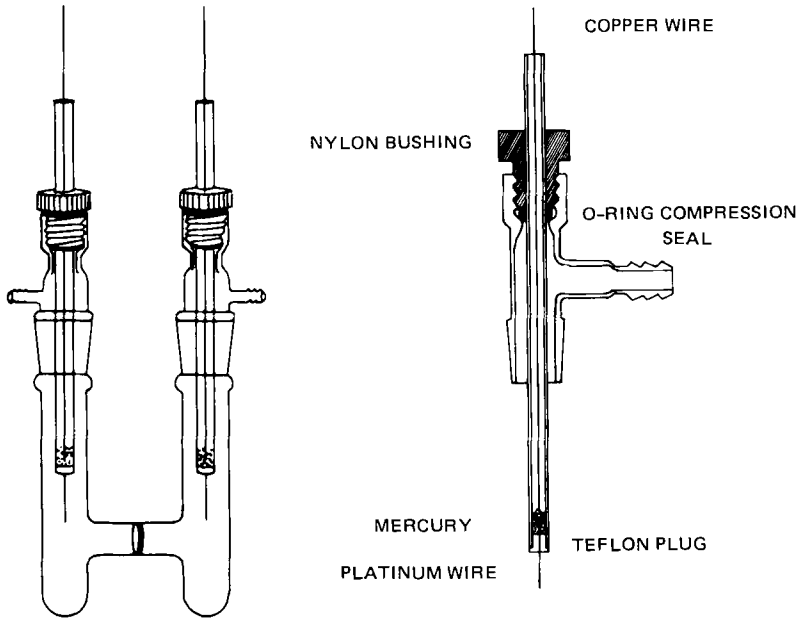


Fig. 3. Cell and electrodes used in the electrocrystallization of organic conductors (*29*).

high-quality crystals ($\sim 0.5 \times 0.5 \times 10$ mm) of TMTSF derivatives are frequently grown. Some typical crystals are shown in Fig. 4.

Before electrocrystallization is initiated the solvent and anionic derivative are placed in the cathode compartment of the cell while the solvent, anionic derivative, and organic donor are loaded in the anode (oxidizing) compartment. Platinum electrodes are then inserted in both compartments and oxidation, with concomitant crystal growth at the anode, is accomplished using either constant voltage or constant current techniques. In the case of $(TMTSF)_2X$, crystals grow on the anode according to the reaction:

$$2n\,(TMTSF) + n\,X^- \xrightarrow{-ne} [(TMTSF)_2X]_n$$

Generally speaking, only one crystalline phase grows when employing TMTSF and an octahedral or tetrahedral anion. However, in the case of ET, as many as four or more different crystallographic phases may form in one growth cycle. As might be expected, sorting out the different ET:X phases is a very complicated task. Using the constant-current technique (current = 1–5 $\mu$A), long shiny black needle-shaped crystals form when TMTSF is used while metallic black crystals of differing morphologies are found when using ET (*8, 31, 106*). In all cases the

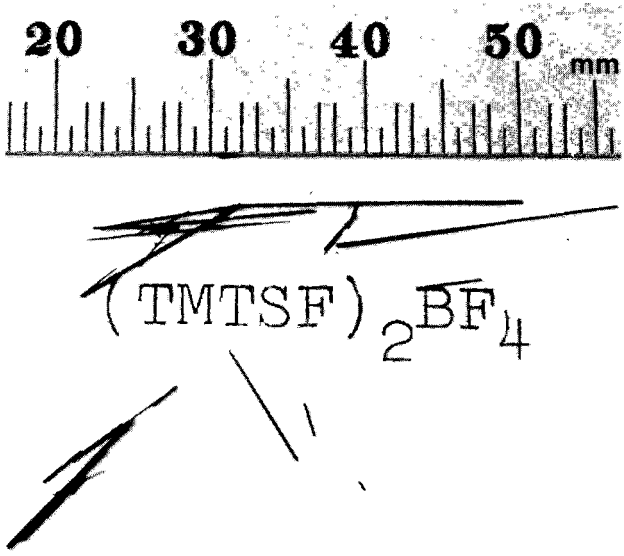


FIG. 4. Photograph of freshly harvested $(TMTSF)_2BF_4$ crystals which were grown using the cell shown in Fig. 3.

crystals formed have a metallic luster but may have electrical properties that vary from insulating to semiconducting to metallic in nature. A detailed description of electrocrystallization, including donor concentration, solvents used, current densities, etc., has been given for $(TMTSF)_2ClO_4$, (*11*) as well as for other TMTSF salts (*20*). A brief review of the preparation and electrical properties of TMTSF derivatives, some with stoichiometries other than the common 2:1 phases, has been published (*10*). The detailed electrocrystallization procedures for $(ET)_2X$ ($X = ReO_4^-$ and $FSO_3^-$) derivatives have also been described (*28*).

## III. Crystal Structures of $(TMTSF)_2X$ and $(ET)_2X$ Conductors

### A. $(TMTSF)_2X$

Understanding the crystal structures of the known organic superconductors is essential because they provide some of the vital insight needed to unravel the variety of physical properties exhibited by these materials. Their understanding also provides a means for varying the electrical properties and for engineering new organic metals. For example, although *all* $(TMTSF)_2X$ compounds possess the same triclinic (space group $P\bar{1}$) crystal structure at room temperature, which is an unusual characteristic of these materials, they may have vastly different properties at low temperature or high pressures. This is demonstrated by the facts that (1) a pressure of 6.5 kbar must be applied to $(TMTSF)_2PF_6$ before it will become superconducting at 0.9 K, (2) $(TMTSF)_2ReO_4$ has an anion-assisted disorder/order transition at 180 K where it loses its metallic properties (unless pressure is applied which suppresses the transition), and (3) $(TMTSF)_2ClO_4$ is the only known *ambient pressure* Se-based superconductor with $T_c = 1.3$ K (*10*). The differences in physical behavior are associated with very minute differences in the crystallographic structure. Thus, although the anion plays no obvious role in the actual conduction process, which occurs through a network of Se–Se interactions (*vide infra*), it does cause pronounced changes in electrical properties which we shall discuss in Section IV.

The crystal structure of $(TMTSF)_2BrO_4$ is shown in Fig. 5 as representative of the series (*32*). The basic architectural feature of the isostructural $(TMTSF)_2X$ salts is the zig-zag columnar stacking of nearly planar TMTSF molecules parallel to the high-conductivity *a* axis (*10, 11, 32–40*). The structures of the salts are different from that of

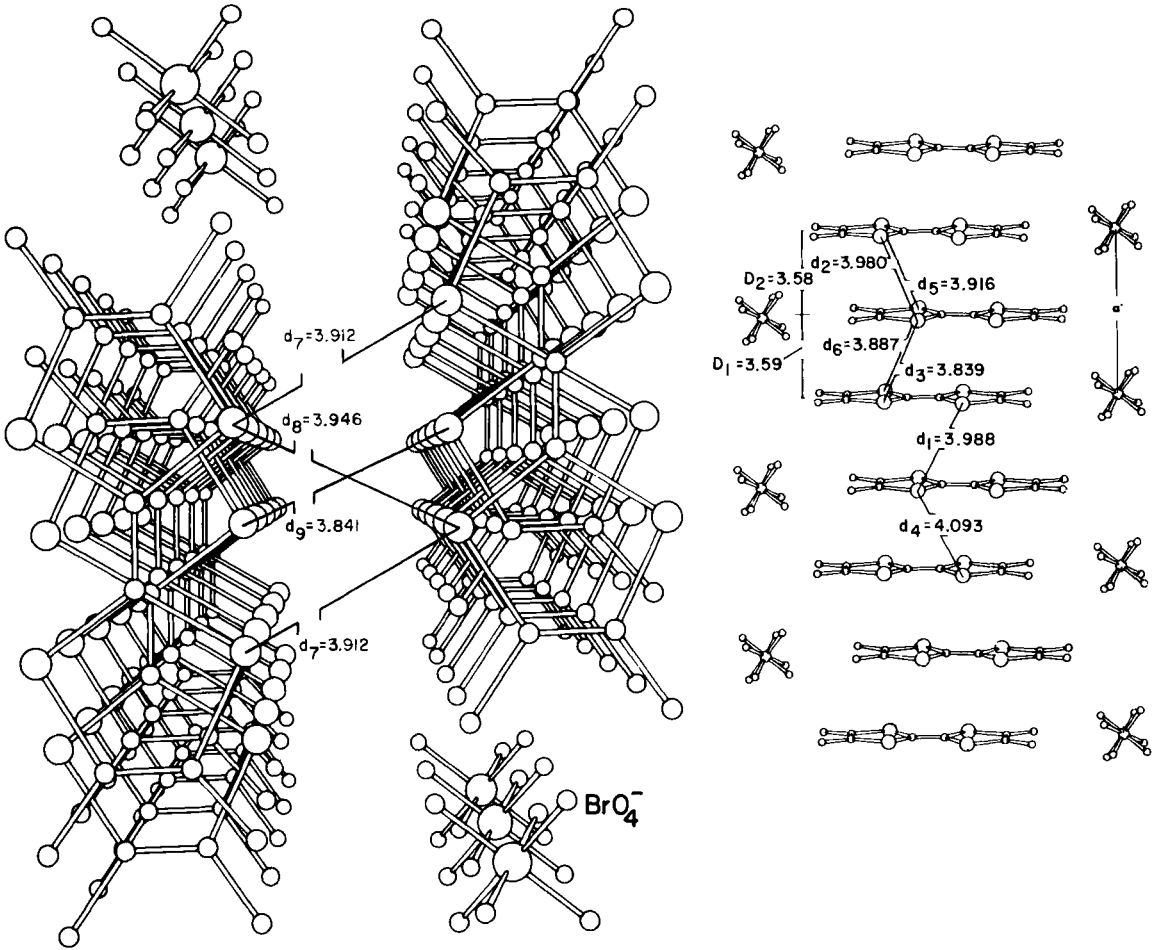


FIG. 5. Perspective views of the crystal structure of $(TMTSF)_2BrO_4$, looking down the stacks along the $a$ axis (left) and perpendicular to them, approximately along the $b$ axis (right). Not all of the oxygen atom positions of the anion, which result from crystallographic disorder, are shown. The Se···Se contact distances ($d$'s) are indicated.

neutral TMTSF itself (*41*). The TMTSF molecules in $(TMTSF)_2X$ salts form stacks along the *a* crystallographic axis, which turns out to be the direction of highest electrical conductivity. These stacks also result in the formation of infinite two-dimensional molecular sheets, which extend in the *a*–*b* plane, with the TMTSF molecules connected through *inter*stack Se · · · Se interactions, thereby providing added "dimensionality" to the system beyond that provided solely by the one-dimensional stacks of TMTSF molecules. However, the TMTSF molecules themselves do not form a three-dimensional network because the sheets are separated along *c* by the anions (X).

Possibly the most important structural feature that has been revealed from crystallographic studies performed at two temperatures (298 and 125 K) is the existence of an "infinite sheet network" (*32*) of Se–Se interactions as shown in Fig. 6. At room temperature the intermolecular *intra-* and *inter*stack Se–Se distances are all similar and have values of 3.9–4.9 Å, compared to the van der Waals radius sum for the selenium atom (*52*) of 4.0 Å. However, as the temperature is lowered (298 → 125 K) rather unusual changes occur, viz. the ratio of the decrease in the *inter*stack:*intra*stack Se–Se distances is not unity but is approximately 2:1 (*32, 40*). Thus, the distances between the "chains" shown in Fig. 6 decrease, on the average, by twice as much as the distances between TMTSF molecules in each stack. This most certainly leads to increased *inter*chain bonding and electronic delocalization through the selenium atom network as the temperature is decreased (*42*).

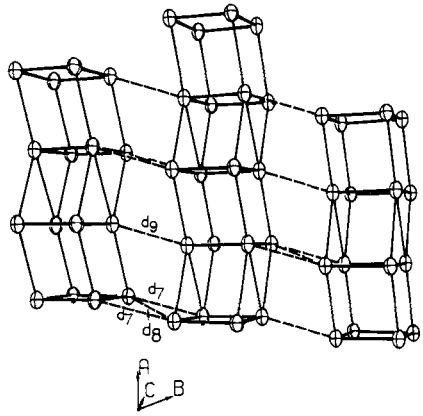


FIG. 6. Representation of the selenium atom "infinite sheet network" in $(TMTSF)_2X$ salts. This network is the main pathway for electrical conduction. Lines connect selenium atoms that are closer than the van der Waals' radius sum (Se · · · Se) of 4.0 Å. Full lines show *intra*stack, broken lines, *inter*stack distances: $d_7$, $d_8$, and $d_9$.

Given the importance of the specific anions for the physical behavior of the $(TMTSF)_2X$ salts it seems worthwhile to dwell upon the influence of their sizes and shapes on the crystallographic properties. Contrary to previous reports, even the centrosymmetric anions $AsF_6^-$ and $PF_6^-$ are in crystallographic disorder with their central atom most likely always residing at the inversion center (1 site) in the triclinic unit cell (*39*). When $X^-$ is highly symmetric (octahedral or tetrahedral), the network of interstack Se–Se distances expands and contracts in a surprisingly predictable fashion as the size of the anion is varied. This network expansion, not surprisingly, is accompanied by systematic changes in the crystallographic unit cell volume. These features are demonstrated in Figs. 7 and 8. We define the anion volume $V_A$ by using effective ionic radii (*43*). Adopting the method of Shannon and Prewitt (*44*) for deriving effective multiatomic radii we define $V_A$ by the volume of the sphere that has the correct multiatomic radius. Hence, $V_A = \frac{4}{3}\pi(r_i + 2r_o)^3$, where $r_i$ is the radius of the inner ion (e.g., Cl in $ClO_4^-$) and $r_o$ is that associated with the outer ion.

By plotting known $V_c$ values for six TMTSF salts (X = $PF_6^-$, $ReO_4^-$, $BrO_4^-$, $ClO_4^-$, $BF_4^-$, and $FSO_3^-$) versus $V_A$, a linear relation between

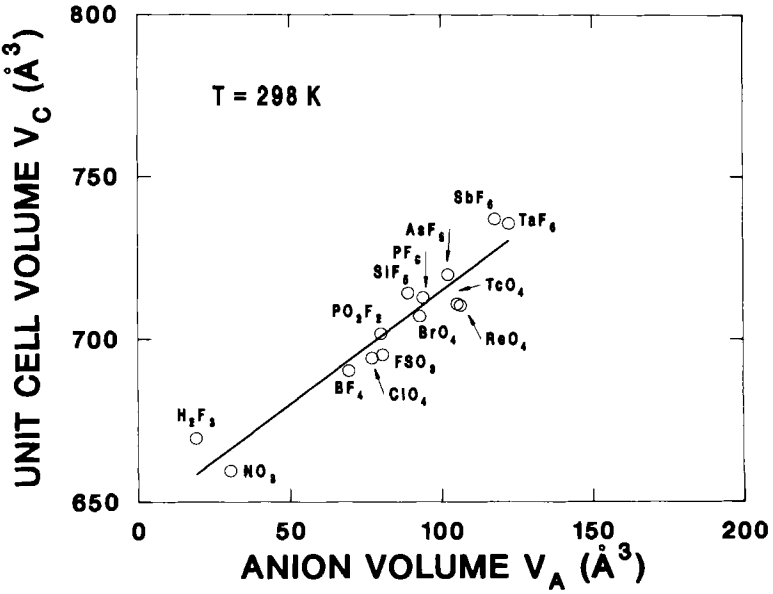


FIG. 7. Plot of unit cell volume $V_c$ of $(TMTSF)_2X$ salts at room temperature vs. anion volume $V_A$.

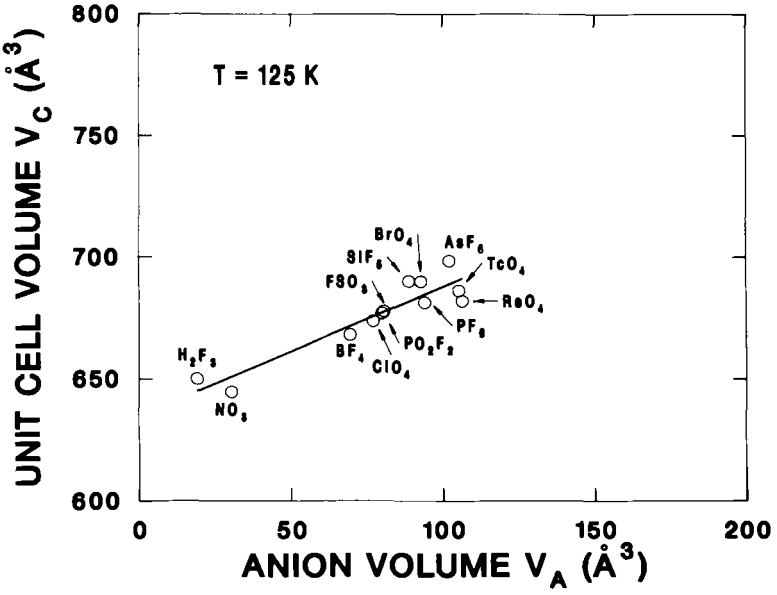


FIG. 8. Plot of unit cell volume $V_c$ of $(TMTSF)_2X$ salts at 120–125 K vs. anion volume $V_A$.

$V_c$ and $V_A$ is observed, both at $T = 295$ K (Fig. 7) and at $T = 125$ K (Fig. 8). This suggests that $V_c$ may be accurately estimated by using a linear least-square fit, to yield a calculated volume (*40*)

$$V_{cp} = 0.65 V_A + 645 \qquad (T = 298 \text{ K})$$

or

$$V_{cp} = 0.42 V_A + 642 \qquad (T = 125 \text{ K}).$$

For example, for $ClO_4^-$ ($r_{Cl}^{7+} = 0.22$ Å and $r_o^{2-} = 1.21$ Å), the calculated $V_c$ is 675 Å$^3$ and the observed $V_c$ is 673.7 Å$^3$ ($T = 125$ K). Concerning bond lengths within an anion, our use of effective radii is justified because the results are identical to those obtained from molecular orbital calculations (*45, 46*). But the empirical effective anion volume, i.e., its contribution to $V_c$, is only about 50% of the calculated $V_A$ [65% (298 K) and 42% (125 K)] of calculated $V_A$. Values of these volumes are given in Table I and we conclude that our approach provides a very good measure of the anion volumes, in particular their relative sizes.

TABLE I

INTERNUCLEAR DISTANCES ($r$) AND ANIONIC VOLUMES ($V_A$) CALCULATED FROM MOLECULAR ORBITAL CALCULATIONS (MO), EFFECTIVE IONIC RADII (EIR), AND COMPARED TO EXPERIMENTAL VALUES (EXP)

| | | Internuclear Distance (Å) | | | $V_A$(Å$^3$) | |
|---|---|---|---|---|---|---|
| Anion | | MO[a] | EIR | EXP[a] | EIR | EXP[b] |
| $H_2F_3$ | | | | | 19 | 25 |
| $NO_3$ | $r_{N-O}$ | 1.277 | 1.28 | 1.22–1.27 | 30 | 20 |
| $BF_4$ | $r_{B-F}$ | 1.380 | 1.42 | 1.40–1.43 | 70 | 45 |
| $ClO_4$ | $r_{Cl-O}$ | 1.542 | 1.44 | 1.41–1.43 | 77 | 49 |
| $FSO_3$ | $r_{S-F}$ | 1.601 | 1.42 | 1.55–1.555 | 81 | 50 |
| | $r_{S-O}$ | 1.459 | 1.48 | 1.424–1.455 | | |
| $BrO_4$ | | | | | 93 | 62 |
| $PF_6$ | $r_{P-F}$ | 1.612 | 1.68 | 1.60–1.63 | 94 | 59 |
| $AsF_6$ | $r_{As-F}$ | 1.744 | 1.76 | 1.59–1.96 | 102 | 74 |
| $TcO_4$ | | | | | 105 | 66 |
| $ReO_4$ | | | | | 106 | 65 |
| $SbF_6$ | $r_{Sb-F}$ | 1.895 | 1.90 | 1.53–1.99 | 118 | 72 |
| $TaF_6$ | | | | | 122 | 91 |
| $CF_3SO_3$ | | | | | 153 | 95 |

[a] Data from refs. *45, 46.*

[b] Room temperature value = $V_C - 645$ Å$^3$.

It appears that the search for new superconducting $(TMTSF)_2X$ derivatives should center around those for which the unit cell volume is close to that of $(TMTSF)_2ClO_4$ [$V_c = 694.3$ Å$^3$ (298 K) and 673.7 Å$^3$ (125 K)]. Thus, the equations and methodology given here are of practical use because, for any imaginable anion, the unit cell volume can be predicted before the salt is prepared. For example, based on the equations above, candidates for superconductivity might be $(TMTSF)_2PO_2F_2$ [$V_{cp} = 675.6$ Å$^3$ (125 K)], $(TMTSF)_2CrO_3F$ [$V_{cp} = 679.1$ Å$^3$ (125 K)], and $(TMTSF)_2WF_6$ [$V_{cp} = 692.4$ Å$^3$ (125 K)]. While $(TMTSF)_2PO_2F_2$ has been prepared (*47, 48*), it undergoes a metal–insulator transition at 137 K (*47*) and pressures up to 15 kbar do not induce superconductivity; the $CrO_3F^-$ anion oxidizes TMTSF and a derivative cannot be prepared (*68*); and $(TMTSF)_2WF_6$ has not yet been prepared but it is expected that pressure would be required to induce superconductivity because of the larger (predicted) unit cell volume compared to that of $(TMTSF)_2ClO_4$.

Important further illuminations of the relationships between the structural and transport properties is provided by crystallographic studies under pressure. As yet, very limited information is available. However, from studies of $(TMTSF)_2PF_6$, the volume compressibility is estimated to be 0.5% $kbar^{-1}$ (*49*). It, therefore, requires ~6 kbar to compress $(TMTSF)_2PF_6$ into the same volume as $(TMTSF)_2ClO_4$, which is in rough agreement with the critical pressure for superconductivity in the $PF_6^-$ compound.

As indicated above, the major structural changes upon cooling involve the interstack Se–Se distances ($d_7$, $d_8$, and $d_9$ in Fig. 6), which are given in Table II. Inspection of the interstack Se–Se contact distances in Table II reveals that upon cooling large decreases in Se–Se distances occur which are as much as 0.30 Å less than the van der Waals radius sum for Se, thus suggesting considerable bonding interaction (*42*). It has also been observed (*40*) that the Se–Se distances are anion dependent, and vary systematically depending on the anion size, suggesting that *correlations* between crystallographic unit cell volumes, which reflect anion size, and interstack Se–Se distances might

TABLE II

INTERSTACK Se–Se CONTACT DISTANCES (Å) AND UNIT CELL VOLUMES (Å$^3$) FOR $(TMTSF)_2X$[a]

| Anion ($X^-$) | | $d_7$ (Å) | $d_8$ (Å) | $d_9$ (Å) | $V_c$ (Å$^3$) |
|---|---|---|---|---|---|
| $AsF_6^-$: | 298 K | 3.9449(9) | 3.9627(11) | 3.9053(13) | 719.9 |
| | 125 K | 3.8159(5) | 3.8861(7) | 3.7894(7) | 695.9 |
| $PF_6^-$ | 298 K | 3.9342(20) | 3.9586(27) | 3.8786(28) | 714.3 |
| | 125 K | 3.7847(14) | 3.8706(22) | 3.7413(22) | 681.3 |
| $ReO_4^-$ | 298 K | 3.902(2) | 3.933(2) | 3.827(2) | 710.5 |
| | 125 K | 3.794(4) | 3.845(5) | 3.699(4) | 681.9 |
| $BrO_4^-$ | 298 K | 3.9118(9) | 3.9457(14) | 3.8411(13) | 707.2 |
| | 125 K | 3.8149(8) | 3.8618(12) | 3.7216(11) | 689.8 |
| $FSO_3^-$ | 298 K | 3.8676(7) | 3.9516(11) | 3.7815(9) | 695.3 |
| | 125 K | 3.7565(5) | 3.8382(8) | 3.6601(7) | 677.7 |
| $ClO_4^-$ | 298 K | 3.8653(14) | 3.9553(24) | 3.7783(20) | 694.3 |
| | 125 K | 3.7596(5) | 3.8485(9) | 3.6549(8) | 673.7 |
| $BF_4^-$[b] | 298 K | 3.850 | 3.978 | 3.743 | 690.4 |
| | 125 K | 3.7526(11) | 3.8792(17) | 3.6394(15) | 668.1 |

[a] Estimated standard deviations are in parentheses.

[b] Values at 298 K were given without estimated standard deviations (*109*).

exist. As shown in Fig. 9 there is a very striking correlation between the anion volume $V_A$ (and hence, unit cell volume $V_c$) and the average interstack Se–Se distance [$d_{avg} = (2d_7 + d_9)/3$] in $(TMTSF)_2X$ metals and these structural features also correlate well with the observation of pressure-induced superconductivity in the majority of these systems.

Within the series of octahedral and tetrahedral anions the $ClO_4^-$ anion has a small volume $V_A$, and also a very small $d_{avg}$ and $V_c$. It is, therefore, tempting to make $(TMTSF)_2X$ salts with even smaller anions than $ClO_4^-$, and examples of such ions are the triangular (pancake-shaped) $NO_3^-$ and (banana-shaped) $H_2F_3^-$. It is now interesting to compare the unit cell volumes $V_c$ and the interstack distances $d_{avg}$ of these compounds to what is expected from the larger and more symmetric anions treated above. From Figs. 7 and 8 it appears that $V_c$ behaves regularly, i.e., it follows the usual linear behavior versus $V_A$. However, the $d_{avg}$ value when $X = H_2F_3^-$ departs appreciably from the expected dependence as is shown in Fig. 9. This deviation is related to the fact that although the very small anions $NO_3^-$ and $H_2F_3^-$ do make the unit cell volume smaller than that for $X = ClO_4^-$, the interstack selenium atom network does not contract accordingly. It is tempting to

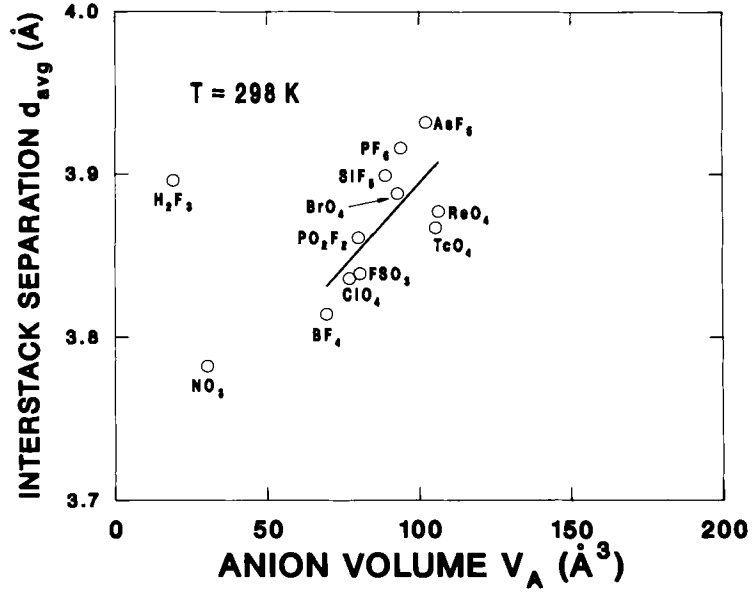


FIG. 9. Average interstack distance, $d_{avg}$ (see text), in $(TMTSF)_2X$ salts at room temperature vs. anion volume $V_A$.

relate this structural observation with the fact that superconductivity is not observed in $(TMTSF)_2NO_3$ and $(TMTSF)_2H_2F_3$ (*50*).

Another possibly important correlation between crystal structure and the occurrence of superconductivity in $(TMTSF)_2X$ materials may be related to short cation–anion contact distances which occur through Se---F or Se---O interactions (*51*). In the $(TMTSF)_2X$ series superconductivity has definitely been observed for $X = PF_6^-$, $AsF_6^-$, $TaF_6^-$, $SbF_6^-$, $ReO_4^-$, and $ClO_4^-$; in the latter case only is superconductivity observed at ambient pressure. The van der Waals contact distances for Se–Se, Se–F, and Se–O are 4.00, 3.35, and 3.40 Å, respectively (*52*). The cation–anion contacts through Se–(F,O) are given in Table III and they reveal very short contact distances except for $(TMTSF)_2NO_3$, which does not undergo a superconducting transition. Since the short contacts lie approximately in the *c* direction, Parkin *et al.* used these observations to suggest that it is the length of the *c* axis that determines the critical pressure for superconductivity (*104*). However, compressibility studies show that it would require a much higher pressure to compress the *c* axis of $(TMTSF)_2PF_6$ into that of $(TMTSF)_2ClO_4$ than the pressure needed for superconductivity (*49*). Hence, the *c* axis criterion is unlikely to play a determining role for the occurrence of superconductivity in $(TMTSF)_2X$ salts.

A third interesting aspect concerning the detailed structures of $(TMTSF)_2X$ materials and the role the anions play, in addition to the correlations previously described and the finding of short Se–(F,O) anion distances discussed above, is the observation that the peripheral atoms of the anions, viz. $AsF_6^-$, $PF_6^-$, and $ClO_4^-$, are involved in weak van der Waals interactions with the hydrogen atoms of the methyl groups in $(TMTSF)_2X$, indicating interactions resembling weak hydrogen bonds (*39, 53*). For example, the immediate nearest neighbor

TABLE III

SHORT CATION–ANION Se–(O,F) DISTANCES IN $(TMTSF)_2X$ MATERIALS AT ROOM TEMPERATURE

| | X | | | | | |
|---|---|---|---|---|---|---|
| | $NO_3^-$ | $ClO_4^-$ | $ReO_4^-$ | $PF_6^-$ | $TaF_6^-$ | $PO_2F_2^-$ |
| Se–(O,F) Å | 3.94 | 3.34 | 3.16 | 3.23 | 3.09 | 2.91[a] |

[a] This short contact, which is the shortest Se–O distance observed in any $(TMTSF)_2X$ salt, arises because below the metal–insulator transition at 137 K (*47*) the anion is shifted off the center of symmetry resulting in a crystallographic disorder (*48*).

environment about the disordered (*39*) octahedral $AsF_6^-$ anion in $(TMTSF)_2AsF_6$ reveals a nearly isotropic (symmetric) sea of nearby ($d < 2.6$ Å) hydrogen atoms (see Fig. 10) arising from the fact that in these materials the anion resides in a "methyl-group H-atom cavity" (*53*).

In contrast, the tetrahedral $ClO_4^-$ anion in $(TMTSF)_2ClO_4$ possesses a very asymmetric methyl-group hydrogen atom environment as shown in Fig. 11. This asymmetric distribution of oxygen atom to methyl-group hydrogen atom [$H_2C–H \cdots O–ClO_3^-$] bonding interactions results in a "pinning" of the anion, which may be associated with the critical anion-ordering phase transition, a necessary prerequisite to superconductivity in $(TMTSF)_2ClO_4$, observed at 24 K using X-ray diffraction techniques (*54*). As illustrated in Fig. 11, the lower relative thermal motion, as observed in their thermal vibration ellipsoids, of O(1) and O(2) compared to O(3) and O(4) undoubtedly results from the greater involvement of O(1) and O(2) in what could be termed "weak H-bond formation." It has also been proposed that the anion-ordering phenomena observed in many $(TMTSF)_2X$ compounds may be associated with methyl-group ordering which occurs at low temperature in these materials (*53*). If this is the case, then the synthesis of new superconducting materials requires anions that interact with the methyl groups in such a fashion that they produce anion-ordered derivatives. It is, perhaps, pertinent to point out that controlling the formation of C–H $\cdots$ X interactions in a crystal is an extremely difficult task.

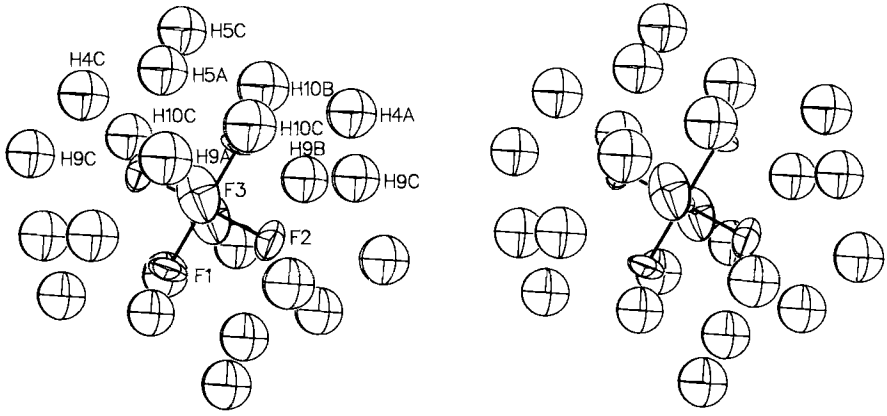


FIG. 10. The H-bonding environment (stereoview) about the $AsF_6^-$ anion, derived from the low-temperature (125 K) X-ray crystal structure of $(TMTSF)_2AsF_6$, is far more symmetrical than that of the $ClO_4^-$ anion (*39*). For clarity the $AsF_6^-$ anion has been drawn in an *ordered* configuration with the fluorine atoms occupying six positions. A disordered model with 12 partially occupied fluorine positions gives similar results.

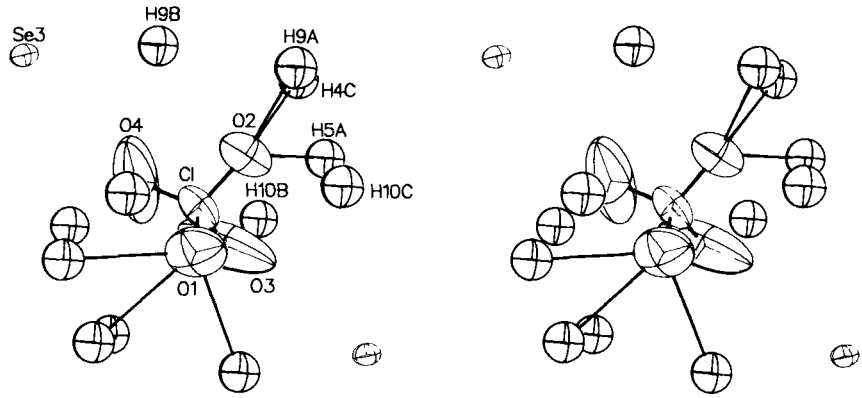


FIG. 11. A stereoview of the ordered $ClO_4^-$ anion environment in the low-temperature (125 K) X-ray-determined crystal structure of $(TMTSF)_2ClO_4$. Short $H_2C-H\cdots O-ClO_3^-$ hydrogen bonding interactions (drawn as faint lines for $O\cdots H < 3.0$ Å) exist for O(1) and O(2), which limit the thermal motion of these atoms and may be responsible for "pinning" the $ClO_4^-$ anion in the lattice (*53*).

As a final point regarding the structure of $(TMTSF)_2X$ conductors, it seems worth mentioning that, contrary to a previous report (*55*), there is no significant dimerization in the (TMTSF) stacks, as indicated by the interplanar distances $D_1$ and $D_2$ given in Table IV (*50*). Such a dimerization could influence the electronic properties, since it would create a gap in the electronic spectrum at the wave-vector $2\mathbf{k}_F(=\pi/a)$,

TABLE IV

INTERPLANAR DISTANCES FOR $(TMTSF)_2X$ SALTS[a]

| Anion $(X^-)$[b] | $D_1$[c] | $D_2$[c] | $\Delta(D_1 - D_2)$ |
|---|---|---|---|
| $AsF_6^-$ | 3.65; 3.57 | 3.62; 3.57 | 0.03; 0.0 |
| $PF_6^-$ | 3.66; 3.59 | 3.63; 3.59 | 0.03; 0.0 |
| $ReO_4^-$ | 3.64; 3.59 | 3.64; 3.56 | 0.0; 0.03 |
| $BrO_4^-$ | 3.63; 3.59 | 3.65; 3.58 | −0.02; 0.01 |
| $FSO_3^-$ | 3.62; 3.58 | 3.63; 3.57 | −0.01; 0.01 |
| $ClO_4^-$ | 3.63; 3.58 | 3.63; 3.57 | 0.0; 0.01 |
| $BF_4^-$ | 3.63; 3.57 | 3.63; 3.55 | 0.0; 0.02 |

[a] The first value is for $T = 298$ K; the second value for $T = 125$ K.

[b] Data from the author's laboratory, except for $X^- = ReO_4^-$, from ref. *110*.

[c] The interplanar distances $D_1$ and $D_2$ are the distances between the best plane for the four Se atoms of a TMTSF molecule.

where $\mathbf{k}_F$ is the Fermi vector. Usually only a gap at $\mathbf{k}_F$ will affect transport properties of a metal, but if Coulomb repulsion between electrons is of importance, the "dimerization gap" is effective and decreases conductivity. With this in mind, it should be noted that both the dimerization (observed from crystallographic studies) and Coulomb repulsion effects (derived from transport measurements) are small in $(TMTSF)_2X$ salts but appear appreciable in the sulfur family of $(TMTTF)_2X$ (TMTTF = tetramethyltetrathiafulvalene).

## B. $(ET)_2X$

Turning now to a discussion of the crystal structures of $(ET)_2X$ conductors, we start by noting that these do not always crystallize with one single type of structure. Therefore, at this time, it is not feasible to carry the analysis of their structure–property relationships to nearly the same degree of detail as was done for the $(TMTSF)_2X$ series.

As an illustration of the structures adopted by the tetrahedral anion materials, the crystal structure of $(ET)_2BrO_4$ is shown in Fig. 12 (*56*). At room temperature it crystallizes with a triclinic unit cell (space group $P\bar{1}$) and this compound is isostructural (*56*) with the pressure-induced superconductor $(ET)_2ReO_4$ (*8, 57*). At first sight, this structure somewhat resembles that of the $(TMTSF)_2X$ materials for the following reason: loosely packed molecular stacks are formed along *a* with the molecular planes placed approximately perpendicular to the stacking axis. The stacks are in close contact along *b* and are separated along *c* by the anions, so that the *ab* planes contain sheets of interacting sulfur atoms.

However, significant differences occur between the $(TMTSF)_2X$ and $(ET)_2X$ structures which are important to point out. Compared to the TMTSF salts the ET donor molecules are far from planar and do not stack in the same zig-zag array as shown in Fig. 5, but clearly in a more complicated array. And a striking difference is observed between the sulfur atom "corrugated sheet network" (*56*) of $(ET)_2X$ ($X = ReO_4^-$ or $BrO_4^-$) (Fig. 13) and the selenium atom sheet network in $(TMTSF)_2X$ (Fig. 6).

It appears that there are no *intra*stack S · · · S contact distances (along the stacks) shorter than the S · · · S van der Waals radius sum of 3.6 Å, either at room temperature or at 120 K. Only between chains are short *inter*stack contacts formed in $(ET)_2X$ ($X = BrO_4^-, ReO_4^-$). Hence, from a structural point of view, these two salts are not quasi-one-dimensional, a fact, however, which does not preclude that the

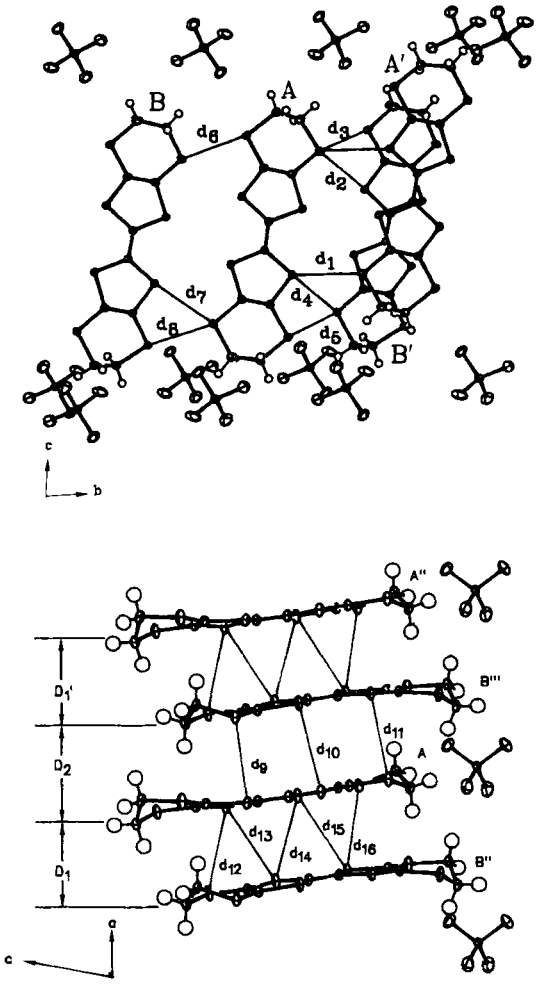


FIG. 12. View of the intermolecular S···S interactions in $(ET)_2BrO_4$. The top figure indicates the *inter*stack S···S contact distances less than the van der Waals sum of 3.60 Å (298/125 K); $d_1 = 3.581(2)/3.505(2)$, $d_2 = 3.499(2)/3.448(2)$, $d_3 = 3.583(2)/3.483(2)$, $d_4 = 3.628(2)/3.550(2)$, $d_5 = 3.466(2)/3.402(2)$, $d_6 = 3.497(2)/3.450(2)$, $d_7 = 3.516(2)/3.434(2)$, and $d_8 = 3.475(2)/3.427(2)$ Å. The S···S contact distances, $d_9$–$d_{16}$ (bottom), are, by contrast, all longer than 3.60 Å even at 125 K. In addition the loose zig-zag molecular packing of ET molecules is such that they are not equally spaced, $D_1 = 4.01/3.95$ Å and $D_2 = 3.69/3.60$ Å. As a result of the (apparently) weak intrastack and strong interstack interactions, $(ET)_2X$ molecular metals are *structurally* different from the previously discovered $(TMTSF)_2X$ based organic superconductors. Almost identical S···S distances and interplanar spacings are observed in $(ET)_2ReO_4$ at both 298 and 125 K. Only theoretical calculations will reveal the extent, if any, of chemical bonding associated with the various S···S distances observed in (ET): X systems.

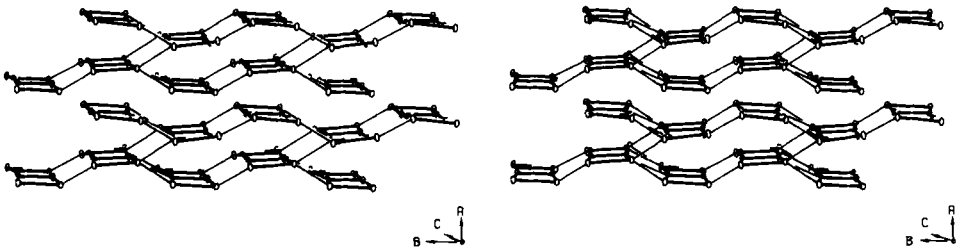


FIG. 13. A stereoview of the short (< 3.60 Å) intermolecular interstack S–S interactions in $(ET)_2ReO_4$ and $(ET)_2BrO_4$ which form a two-dimensional "corrugated sheet" network network (*56*). This network, which is the principal pathway for electrical conduction, is much different from that observed in $(TMTSF)_2X$ salts, but similar to the network of interstack S–S interactions observed in $ET_2(ClO_4)(TCE)_{0.5}$ (*59*).

electronic structure may well be so. The ambient-pressure superconductor $\beta$-$(ET)_2I_3$ has a crystal structure which is markedly similar to the above mentioned $(ET)_2X$ conductors (*58, 102, 106*), in terms of the long *intra*stack and short *inter*stack S · · · S contacts. It is also noteworthy that compared to the $(ET)_2X$ ($X = BrO_4^-$ and $ReO_4^-$) conductors, the molecular stacks in $\beta$-$(ET)_2I_3$ are not perpendicular to any specific crystallographic axis, but rather the [110] direction (see Fig. 14).

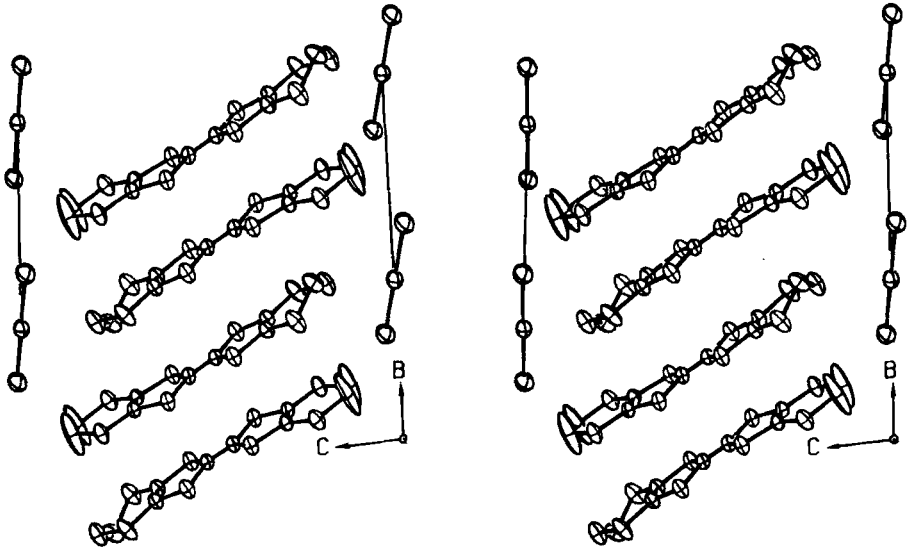


FIG. 14. Molecular packing (stereoview) of ET molecules and linear (centrosymmetric) $I_3^-$ anions in $\beta$-$(ET)_2I_3$. Note that the loose molecular stacks occur in the [110] direction rather than a crystallographic axis as found in $(TMTSF)_2X$ salts.

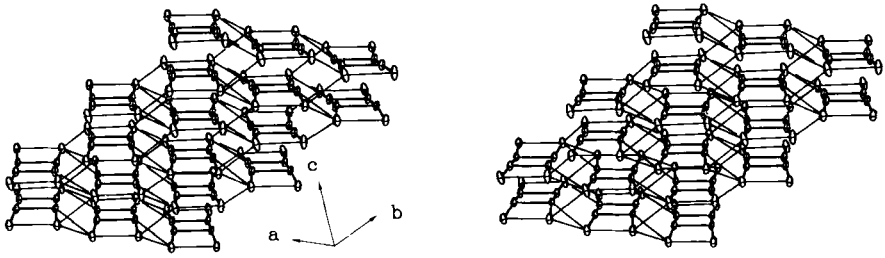


FIG. 15. Stereoview of the "corrugated sheet network" of short *inter*stack S···S interactions (faint lines) between nonplanar and nonparallel ET molecules in $\beta$-$(ET)_2I_3$ at 125 K (90% ellipsoids). For clarity, only the sulfur atoms of ET are shown.

At first sight, $\beta$-$(ET)_2I_3$ bears remarkable resemblance to the 1:2 $M(TCNQ)_2$ salts, where the conducting molecules form stacks of dimers and where the molecules are tilted with respect to the conducting axis. But as pointed out above, one observes mainly short *inter*stack distances compared to the *intra*stack S···S separations, and this superconductor appears to be rather two-dimensional in structure (see Fig. 15).

Finally, it should be noted that exactly the same 2:1 $ET:I_3^-$ stoichiometry results, during electrocrystallization, in the simultaneous formation of two different forms of $(ET)_2I_3$, i.e., the $\alpha$ and $\beta$ forms, respectively. The crystal structure of $\alpha$-$(ET)_2I_3$ (*102, 111*) differs markedly from that of $\beta$-$(ET)_2I_3$ (*58, 102, 106*). Not surprisingly, the electrical properties are also very different with the $\alpha$ form undergoing a metal insulator transition at 135 K (*111*) while the $\beta$ form is the first sulfur-based ambient-pressure organic superconductor (*9, 105, 106, 114*). A most surprising structural feature of $\beta$-$(ET)_2I_3$ is the development, at 200 K and down to at least 11 K, of a novel incommensurate "modulated" structure (*112, 113*) observed for the first time in an organic superconductor. The main features of the modulated structure involve displacements from the "average" crystal structure positions of the $I_3^-$ anion and ET molecules, which have *different* direction and magnitude, viz. 0.281(1) Å for $I_3^-$ and 0.124(3) Å for the ET molecules, respectively (*112, 113*). The modulated structure is shown in Fig. 16 and it must be noted that the resulting local fluctuations of the interatomic S···S distances due to the displacive modulation are very significant and will have to be taken into account in any future theoretical studies of this material.

The same type of corrugated sheet network (see Fig. 17) of short ($d < 3.6$ Å) S···S contacts found in $\beta$-$(ET)_2I_3$ is also observed in

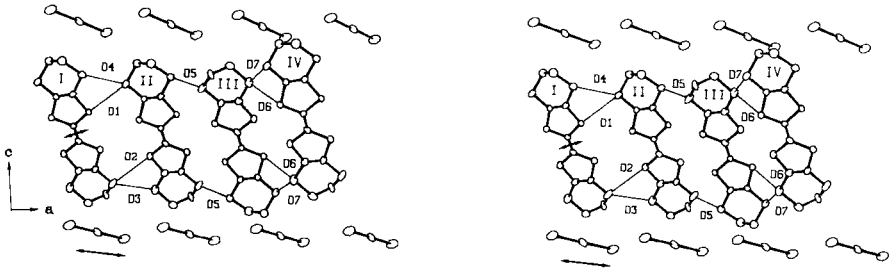


FIG. 16. Stereoview of the molecular packing in $\beta$-$(ET)_2I_3$ on the *ac* plane showing the observed structural modulations of the ET molecules and the $I_3^-$ anions. The allowed displacement vectors of an ET molecule (0.124 Å) and an $I_3^-$ anion (0.281 Å) are indicated by a pair of arrows whose length is approximately five times the magnitude of the observed displacements.

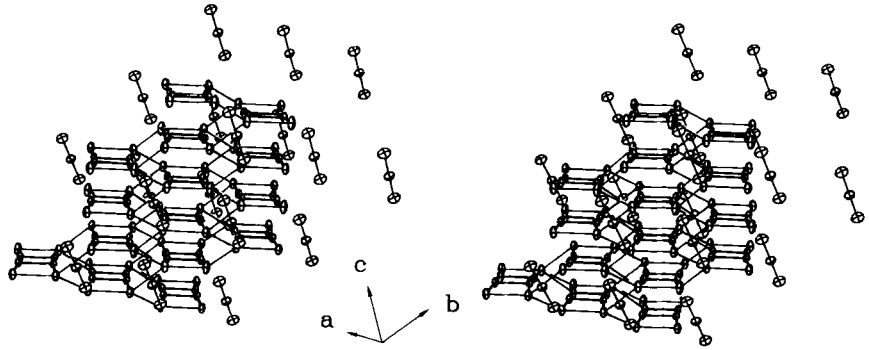


FIG. 17. Stereoview of the novel sandwich or *layered* structure of $\beta$-$(ET)_2IBr_2$ composed of alternating two-dimensional sheets of linear $(Br–I–Br)^-$ anions, between which a "corrugated sheet" network of short *inter*stack S···S interactions is inserted. Only the S atoms of the ET molecules are shown in the network and light lines indicate the *inter*stack ($d_{S\cdots S} < 3.60$ Å) interactions. The $—CH_2$ groups at ET protrude from both ends of the molecule (directly out of the plane of the page) and grasp the $X_3^-$ anions in a pincer hold. Therefore, by varying the length of the $X_3^-$ anion the *inter*stack S···S distances can be directly altered (*108*).

$\beta$-$(ET)_2IBr_2$, with the latter having a much higher superconducting transition temperature of ~2.4–2.7 K (*107, 108*). More important, because the $IBr_2^-$ anion is ~5% shorter than the $I_3^-$ anion, the unit cell volume of the former is less (828.7 vs. 855.9 Å$^3$), with the result that the average *inter*stack S···S contact distance in $\beta$-$(ET)_2IBr_2$ is markedly shorter (0.02 Å) than in $\beta$-$(ET)_2I_3$. Thus, for the first time in any organic system, ambient-pressure superconductivity has been maintained in

two materials having the same donor molecule. The synthesis of $\beta$-$(ET)_2IBr_2$ resulted from a rational and systematic approach involving polyhalide anion displacement with the aim of modifying only slightly the corrugated sheet network in $(ET)_2X$ materials (*108*). This design strategy resulted in direct reduction of the interstack S · · · S distances with anion replacement (see Fig. 17 caption). This occurs because the trihalide anion resides in a cavity formed by $—CH_2$ group hydrogen atoms (*108*) similar to the methyl-group hydrogen atom cavity in $(TMTSF)_2X$ systems. Additional $ET:I_3^-$ salts of presently unknown composition have been reported to be ambient-pressure superconductors with $T_c$ values of 2.5 K (*115, 116*).

For $(ET)_2ClO_4(TCE)_{0.5}$ (TCE = trichloroethane), solvent is incorporated into the structure at positions similar to those occupied by the anions, i.e., separating the sheets of ET molecules (*59*). For this structure definite stacks cannot be identified at all, and, as a consequence, the electronic structure is also very two-dimensional. It is not unlikely that this structure (triclinic with space group $P\bar{1}$) is also adopted by $(ET)_2ReO_4(THF)_{0.5}$ with the only difference being that the solvent here is THF (tetrahydrofuran) (*57*).

As examples of an (ET) conductor with clearly separated stacks, we mention $\beta$-$(ET)_2PF_6$ (*60*) and $(ET)_2AsF_6$ (*103*). They have structures which clearly resemble those typical of the earlier mentioned $M(TCNQ)_2$ conductors and while $\beta$-$(ET)_2PF_6$ undergoes a metal–insulator transition at 297 K (*60*), the same type of transition occurs above 125 K in $(ET)_2AsF_6$ (*103*).

It is noteworthy that the $\beta$-$(ET)_2PF_6$ structure was indeed what one might have predicted for both the $(TMTSF)_2X$ and $(ET)_2X$ salts, based on the analogy between the 2:1 conductors and the previously studied 1:2 TCNQ conductors. Organic superconductivity would probably not have existed if this structural prediction had come true!

We now turn to a discussion of "anion ordering" phenomena in organic conductors in order to better understand the structural transitions often associated with them.

### C. X-Ray Diffuse Scattering Studies of Anion Ordering

Almost two decades ago theoreticians predicted that in a quasi-one-dimensional metal, characterized as having a one-dimensional gas of weakly interacting electrons, instabilities could arise leading to transitions to various ground states, such as charge density wave (CDW), spin density wave (SDW), or superconducting (*61*). Previously, it had been predicted that electron–phonon coupling in a one-dimensional

metal would lead to a CDW state (the Peierls instability) (*6*), and in this case a structural distortion accompanies the formation of an insulating state. In a simple case such as that which occurs in one-dimensional platinum chain systems (*62*), the lattice instability is produced by the softening of a phonon branch at wave vectors of component $2\mathbf{k}_F$ ($\mathbf{k}_F$ is the Fermi wave vector) in the direction of the chains, thereby forming a Kohn (*63*) anomaly in the phonon spectrum.

Because the amplitude of the lattice distortion in the Peierls insulator is very small, the X-ray scattering associated with it is weak. Furthermore the one-dimensional nature of this distortion gives rise to diffuse Bragg planes instead of the usual well-defined Bragg reflections. These two facts have led to the development of a special diffuse X-ray photographic technique often referred to as the "monochromatic Laue technique" or XDS (for X-ray diffuse scattering) (*64*).

For $(TMTSF)_2X$ salts the one-dimensional lattice distortion seems to play a less important role than in other quasi-one-dimensional conductors although faint diffuse $2\mathbf{k}_F$ scattering has been observed (*64–66*). Therefore, the usual Peierls instability is not (or only weakly) active. This is easy to understand in the case of centrosymmetric anions in $(TMTSF)_2X$ ($X = PF_6^-, AsF_6^-, SbF_6^-, TaF_6^-$) since they undergo phase transitions to an antiferromagnetic SDW ground state (*66, 67*), a transition which according to theory does not involve electron–phonon coupling. Under applied pressure the SDW state is suppressed resulting in a superconducting ground state (see Section IV). Hence, for centrosymmetric anions, no new structural features appear at low temperatures.

However, the $(TMTSF)_2X$ derivatives containing noncentrosymmetric anions ($X = ClO_4^-, ReO_4^-, FSO_3^-, H_2F_3^-, BrO_4^-$, and $NO_3^-$) show structural phase transitions at relatively high temperatures compared to the temperatures associated with magnetic (SDW) or superconducting transitions (*69*). These phase transitions are generally associated with anion-ordering phenomena. In this regard it should be remembered that for the noncentrosymmetric anion cases the anion is located at an inversion center (space group $P\bar{1}$), resulting in orientational disorder of the anion at ambient temperature, and XDS studies show that as the temperature is reduced, anion-ordering phase transitions occur (*69*). The transition temperatures, associated wave vectors, and superstructure unit cells are given in Table V (*58, 65, 70–78*).

With the exception of $X = NO_3^-$ and $ClO_4^-$, these compounds exhibit a doubling of their crystallographic axes at the phase transition corresponding to a superstructure with wavevector (1/2, 1/2, 1/2) or ($2\mathbf{k}_F$, 1/2, 1/2). This has the usual symmetry of the

TABLE V

SUPERSTRUCTURES IN $(TMTSF)_2X$ AND $(ET)_2X$ SALTS

| Salt | Anion symmetry | Transition temperature $T_c$ (K) | Wave vector[a] | Unit cell[a] | References |
|---|---|---|---|---|---|
| $(TMTSF)_2H_2F_3$ | | 63 | 1/2, 1/2, 1/2 | 2a, 2b, 2c | *65* |
| $(TMTSF)_2NO_3$ | Triangular | 41 | 1/2, 0, 0 | 2a, b, c | *74, 78* |
| $(TMTSF)_2ClO_4$ | Tetrahedral | 24 | 0, 1/2, 0 | a, 2b, c | *70–72* |
| $(TMTSF)_2BrO_4$ | Tetrahedral | ~250 | 1/2, ?, ? | 2a, ?, ? | *73* |
| $(TMTSF)_2ReO_4$ | Tetrahedral | 177 | 1/2, 1/2, 1/2 | 2a, 2b, 2c | *74–76* |
| $(TMTSF)_2FSO_3$ | | 88 | 1/2, 1/2, 1/2 | 2a, 2b, 2c | *76, 77* |
| $(ET)_2ReO_4$ | Tetrahedral | >300 | 0, 1/2, 0 | a, 2b, c | *8* |
| $(ET)_2ClO_4 \cdot (TCE)_{0.5}$ | Tetrahedral | ≃200 | 1/2, 1/2, 1/2 | 2a, 2b, 2c | *80* |

[a] Referred to the room-temperature $(TMTSF)_2X$ unit cell. [Also for $(ET)_2ClO_4$ and $(ET)_2ReO_4$].

Peierls distortion. A metal–insulator transition occurs simultaneously with the lattice ordering and, as such, the ground state is indistinguishable from a CDW. But the lack of one-dimensional XDS above the transition suggests that the anions play a direct role in establishing the ground state. The two salts with anomalous superstructures also have peculiar electronic properties. Thus, $(TMTSF)_2NO_3$ with its (1/2, 0, 0) superstructure has an SDW ground state and $(TMTSF)_2ClO_4$ with its (0, 1/2, 0) superstructure becomes superconducting only when *slowly cooled* through the anion-ordering transition at 24 K (*70–72*).

Except in the case of $(TMTSF)_2ClO_4$, the only ambient-pressure organic superconductor based on TMTSF, the period of the *a* axis (organic molecule chain axis), doubles at the structural transition. For $(TMTSF)_2ClO_4$ this is an important observation considering the band structure of these materials since $0.5a^*$ ($a^*$ is the reciprocal lattice vector) corresponds to $2\mathbf{k}_F$ for the one-dimensional electron system, i.e., one electron is shared by two molecules in the TMTSF molecular chain. This could lead to the possible opening of a gap at the Fermi level thereby leading to an insulating state. Again, $\mathbf{k}_F$ is the in-chain Fermi wave vector for independent (or weakly interacting) electrons. However, $(TMTSF)_2ClO_4$ undergoes a transition which may be characterized as being of the $4\mathbf{k}_F$ wave vector type which could result from another type of instability of the electron gas arising from Coulomb interaction between electrons. This $4\mathbf{k}_F$ instability can be coupled to the lattice and induce the softening of the $4\mathbf{k}_F$ phonon. However, the lack of

other evidence of strong Coulomb interactions (not the least that superconductivity occurs) suggests a nonelectronic origin of the superstructure. As discussed earlier, in *slowly cooled* (R = "relaxed state") samples only, anion-ordering is a precursor to superconductivity and if samples are cooled suddenly (Q = "quenched state") superconductivity does not develop (*78*). Thus, fast cooling of the sample suppresses superconductivity and stabilizes the SDW ground-state and associated antiferromagnetism. The situation is not yet well understood in terms of the detailed structural changes in $(TMTSF)_2ClO_4$ and this is a topic of intense investigation. In the only other detailed XDS study, of $(TMTSF)_2ReO_4$, the situation is complicated because the $ReO_4^-$ tetrahedra are both ordered below the 176 K phase transition and displaced from their centrosymmetric high-temperature position, and this is accompanied by a "$2\mathbf{k}_F$" distortion of the TMTSF stack (*76, 79*). It should be noted that from a crystallographic point of view, it is often technically difficult to arrive at a refined crystal structure based on both the usual strong reflections and the very weak superstructure reflections.

The similarity between the $(TMTSF)_2X$ salts and $(ET)_2ReO_4$ makes it interesting to look into its structure using as a reference point the room-temperature structure of a $(TMTSF)_2X$ salt. As shown in Table V the room-temperature structure of $(ET)_2ReO_4$ resembles the (0, 1/2, 0) superstructure i.e., that of $(TMTSF)_2ClO_4$ below 24 K. However, transport measurements suggest a new ordering in $(ET)_2ReO_4$ at 81 K, so the analogy is not entirely clear between the structural characteristics of the two superconductors.

Diffuse X-ray scattering experiments reveal a superstructure in $(ET)_2ClO_4(TCE)_{0.5}$ below 200 K of wavevector (1/2, 0, 1/2) which is associated with anion ordering (*80*). When compared to the $(TMTSF)_2X$ structure, it corresponds to a transition from (0, 1/2, 0) at high temperatures to (1/2, 1/2, 1/2) at low temperature but without any noticeable signatures in conductivity or susceptibility. Hence, in this case, where the two basic structures of $(ET)_2ClO_4(TCE)_{0.5}$ and of $(TMTSF)_2X$ are very different, there is no analogy between the effects of their superstructures.

In conclusion, XDS studies of numerous TMTSF systems have provided a great deal of information on the nature of the anion-ordering transitions that occur at various temperatures. However, detailed single-crystal structural analyses are still required in order to determine the precise structural changes associated with these transitions.

## IV. Electrical Conduction

Despite the great similarity in crystallographic structures of $(TMTSF)_2X$ compounds, their electronic properties vary considerably. This is clear from Fig. 18, where the electrical resistivities of some salts are shown as functions of temperature. By comparison to Fig. 2, one finds that the TMTSF molecule is able to reproduce almost all previously studied molecules in giving highly conducting salts with a great variation in metal–insulator transition temperatures ($T_{MI}$) and even superconductivity (at $T_s$). This conclusion contradicts former suggestions that mostly molecular features are responsible for the variation of solid-state properties, because in $(TMTSF)_2X$ compounds identical molecules in very similar crystallographic environments behave quite differently.

The situation in (ET):X salts is different, since they form very different crystallographic structures. Even the same anion may give rise to a multiplicity of crystallographic phases as demonstrated by

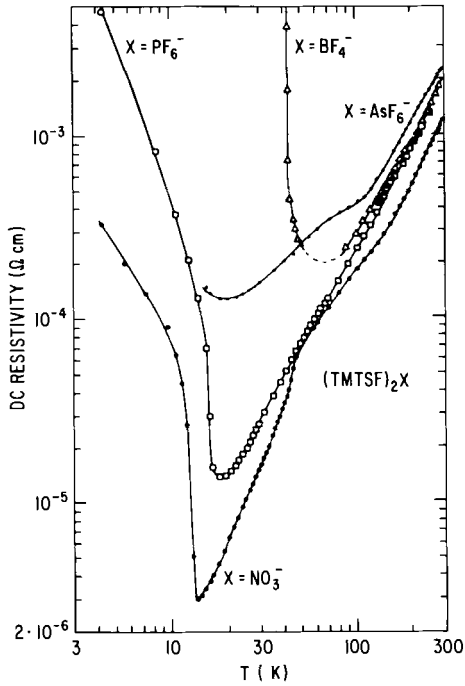


FIG. 18. The electrical resistivities of selected $(TMTSF)_2X$ salts, having anions of various geometries, at ambient pressure (redrawn from ref. *81*).

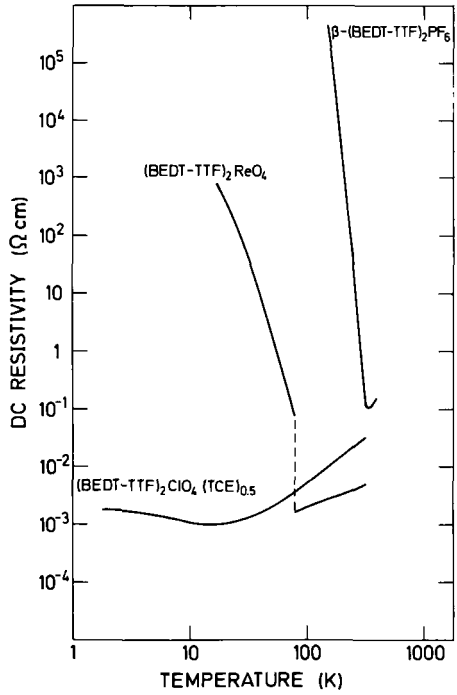


FIG. 19. The electrical resistivities of selected $(ET)_2X$ salts at ambient pressure. Both $\beta$-$(ET)_2I_3$ and $\beta$-$(ET)_2IBr_2$ (not shown) are ambient pressure superconductors with $T_c = 1.5$ and 2.7 K, respectively.

$X = ReO_4^-$, for which four phases have been found. It is, therefore, not astonishing that (ET):X salts have different conduction properties as shown in Fig. 19. The fact that $\beta$-$(ET)_2I_3$ and $\beta$-$(ET)_2IBr_2$ are the second and third ambient-pressure organic superconductors, respectively, and that one phase of $(ET)_2ReO_4$ becomes superconducting under pressure, make the other phases extremely interesting from the point of view of addressing the following question: Which features of the crystallographic environment provide the grounds for superconductivity in an organic conductor? We now turn to this question.

## A. Resistivity along the Chains

### *1.* $(TMTSF)_2X$ *Salts*

The usual features of the electrical resistivities of $(TMTSF)_2X$ compounds shown in Fig. 18 are as follows. The room-temperature value

along the needle axis is typically $\rho_a = 1.5 \times 10^{-3}$ Ω cm (*75, 81*). This is very similar to the value for TTF-TCNQ and somewhat higher than the best conducting organic salt HMTSF-TNAP (TNAP = tetracyanonaphthalene) ($0.5 \times 10^{-3}$ Ω cm) (*82*). The temperature dependence of the resistivity follows an approximate $T^2$ behavior typical of organic conductors when the temperature is above the electronic transition temperatures, $T_{MI}$ or $T_s$. In the cases where the anion-ordering transition at $T_0$ described above does not coalesce with the electronic transition, it results in a small deviation from the $T^2$ dependence of the resistivity.

Below the electronic-transition temperature $T_{MI}$ or $T_S$ the properties change from metallic to either semiconducting ($X = PF_6^-$, $SbF_6^-$, $BF_4^-$, $FSO_3^-$, $ReO_4^-$, $H_2F_3^-$] (*65, 75, 77, 81, 84, 85*) or superconducting ($X = ClO_4^-$) (*85*), where the electronic density of states in both cases is characterized by an energy gap 2Δ. Although it cannot be concluded from the electrical conductivity, we note that the semiconducting salts fall into two classes. One contains the usual dielectric semiconductors [$X = ReO_4^-$ (*81*), $FSO_3^-$ (*77*), $BF_4^-$ (*65*), and $H_2F_3^-$ (*85*)] and they may be characterized as anion-assisted Peierls insulators, since their properties in many respects are like those of the Peierls CDW insulator; but some aspects of their behavior can only be understood as stemming from a direct influence of the anions. The other class of semiconductors has an antiferromagnetic ground state often referred to as the SDW; it contains salts of anions ($X = SbF_6^-$, $AsF_6^-$, $PF_6^-$, and possibly also $NO_3^-$) (*10*). Published values of the activation energy Δ are given in Table VI.

The classification given above is documented to varying degrees for the different compounds. Compelling evidence exists for $(TMTSF)_2ClO_4$ (superconductor), $(TMTSF)_2ReO_4$ (dielectric semiconductor), and $(TMTSF)_2PF_6$ (magnetic semiconductor), so that these salts may be considered as prototypes for the three kinds of low-temperature behavior of the regularly behaving $(TMTSF)_2X$ salts.

Some salts show behaviors which are different from that described above; but most of these have not been well characterized. For example, for $X = BrO_4^-$, which has only recently been well studied, anion disorder seems to lead to localized electronic states (*85*).

### 2. $(ET)_2X$

The electrical resistivities in the molecular stacking direction of some (ET):X salts are shown in Fig. 19. The first material studied, $(ET)_2ClO_4(TCE)_{0.5}$, has a room-temperature value of $4 \times 10^{-2}$ Ω cm

TABLE VI

CONDUCTION CHARACTERISTICS OF $(TMTSF)_2X$ AND $(ET)_2X$ SALTS

| X | $V_A$ (Å$^3$) | $V_c$ (Å$^3$) | $T_o$ (K) | $T_{MI}$ (K) | Δ (meV) | $P_c$ (kbar) | $T_s$ (K) |
|---|---|---|---|---|---|---|---|
| | | | **$(TMTSF)_2X$** | | | | |
| $H_2F_3$ | 10 | 669.6 | 63 | 63[b] | — | — | — |
| $NO_3$ | 30 | 659.5 | 41 | 12[c] | — | — | — |
| $BF_4$ | 70 | 690.4 | 40 | 40[b] | — | — | — |
| $ClO_4$ | 77 | 694.3 | 24 | — | — | 0 | 1.4 |
| $FSO_3$ | 81 | 695.8 | 87.5 | 86[b] | 47 | ~7 | 1.4 |
| $BrO_4$ | 93 | 707.2 | ≃250 | ≃220[c] | — | — | — |
| $PF_6$ | 94 | 712.9 | — | 12[c] | 2.0 | 6.5 | 0.9 |
| $AsF_6$ | 102 | 719.9 | — | 12[c] | 2.0 | 12 | 0.9 |
| $TcO_4$ | 105 | 711.0 | — | — | — | — | — |
| $ReO_4$ | 106 | 710.5 | 177 | 182[b] | 83 | 9.5 | 1.0 |
| $SbF_6$ | 118 | 737.0 | — | 17[c] | | 11 | 0.8 |
| $TaF_6$ | 122 | 735.6 | — | 11[c] | 1.8 | 12 | 0.8 |
| $CF_3SO_3$ | 153 | 739.5 | ≃280 | 280[b] | — | — | |
| | | | **$(ET)_2X$** | | | | |
| $ClO_4(TCE)_{0.5}$ | — | 1684 ($Z = 2$) | | — | — | — | — |
| $PF_6(\alpha)$ | 94 | 794.3 | | — | 54 | — | — |
| $PF_6(\beta)$ | 94 | 3256.4 ($Z = 4$) | | 297 | 276 | — | — |
| $ReO_4$ | 106 | 1565 ($Z = 2$) | | 81 | 45 | 4–6 | 1.3 |
| $I_3(\beta)$ | | 855.9 | | — | — | 0 | 1.4 |
| $IBr_2(\beta)$ | | 828.7 | | — | — | 0 | 2.7 |
| $AsF_6$ | 102 | 3274 | | 125 | — | — | — |

[a] $V_A$ and $V_c$ are the calculated anion volume and measured unit cell volume, $T_o$ is the anion-ordering temperature, $T_{MI}$ is the metal–insulator transition temperature, Δ is the activation energy, $P_c$ is the critical pressure, and $T_s$ is the superconducting transition temperature.

[b] Ground State: anion-assisted charge density wave.

[c] Ground State: spin density wave.

decreasing to about $1 \times 10^{-3}$ Ω cm at $T = 16$ K (*31*). At this temperature the resistivity goes through a broad minimum rising to $1.5 \times 10^{-3}$ Ω cm at the lowest temperatures. This situation is similar to what has been observed in HMTSF-TCNQ under pressure (*86*) and in HMTSF-TNAP (*82*) (HMTSF = hexamethylenetetraselenafulvene).

In the (ET):$ReO_4$ salts the conductivity varies (*8, 57*). The 2:1 salt, which becomes superconducting under pressure, has a sharp metal–insulator transition at 81 K whereas the 3:2 salt has a broader transition at a similar temperature. In the $2{:}1{:}\frac{1}{2}$ salt (where "$\frac{1}{2}$" indicates incorporation of $\frac{1}{2}$ solvent molecule of THF per formula unit) there is no indication of a transition from the conductivity data.

A third 2:1 salt, $\beta$-$(ET)_2PF_6$, shows a usual Peierls instability, as judged from the resistance data of Fig. 19, with an activation energy of 230 meV (*60*). In fact, it looks much like the classical platinum chain conductor $K_2[Pt(CN)_4]Br_{0.3}\cdot 3.2H_2O$ (KCP) (*62*) as do some of the structurally similar $M(TNCQ)_2$ conductors (*2*). It appears that $\alpha$-$(ET)_2PF_6$ has an activated conductivity over the entire temperature region with a low activation energy of 50 meV (*87*). In terms of the optical conductivity derived from polarized specular reflectance data, $\beta$-$(ET)_2I_3$ exhibits, for the first time in an organic conductor, a "cross-over" from one-dimensional behavior at 298 K to three-dimensional behavior at 40 K (*12*).

Finally, the resistivity characteristics of the ambient-pressure superconductor $\beta$-$(ET)_2I_3$ resemble those of $(TMTSF)_2ClO_4$ a great deal except for the much higher $T_c$ of the triiodide salt [its room temperature value is 0.03 $\Omega$ cm (*9, 105, 106, 114*)].

### *3. Discussion*

The ratio $k_BT_{MI}/\Delta$ can be used to illuminate the anisotropy of the electronic structure in a quasi-one-dimensional material. The ratio is 0.567 in the mean field (or molecular field) approximation which holds fairly well for three-dimensional instabilities (e.g., BCS superconductivity); but it approaches zero as the dimensionality goes to unity. With $k_B = 0.086$ meV/K the values of Table VI yield results for $k_BT_{MI}/\Delta$ close to 0.567 for $(TMTSF)_2X$, suggesting that these salts are not very one dimensional. However, the lack of a transition in $(ET)_2ClO_4(TCE)_{0.5}$ should not be confused with extreme one dimensionality. Rather, this compound would appear to be so slightly anisotropic that the one-dimensional instabilities which give rise to the transitions are not active. The extraordinary variation of conductivity behavior of $(TMTSF)_2X$ and (ET):X salts at ambient pressure makes the two donor molecules involved unique. In the metallic phase at high temperature they behave much like previously studied organic conductors apart from the possible features at the anion-ordering temperature $T_o$. But their low-temperature behavior has provided novel superconductivity, spin density waves, and anion-assisted Peierls insulators to condensed-matter physics. Measurements of the resistivity itself contributes to the characterization of these phases by giving information about the electronic and ionic transition temperatures $T_{MI}$, $T_s$, and $T_o$, respectively, and the semiconducting gap parameter $\Delta$ below $T_{MI}$. Values for the different salts are given in Table VI.

## B. Conduction Anisotropy

### 1. $(TMTSF)_2X$ *and* $(ET)_2X$

The electrical resistivity in directions other than the molecular stacking axis has been measured in a few cases. In $(TMTSF)_2PF_6$ one finds $\rho_a:\rho_{b'}:\rho_{c^*} \simeq 1:200(3000):3 \times 10^4(10^6)$, where numbers in parentheses refer to $T = 20$ K, i.e., just above the transition (*88*). Here $b'$ is a vector in the $ab$ plane perpendicular to $a$, and $c^*$ is the reciprocal lattice vector orthogonal to the same plane. The situation in $(TMTSF)_2PF_6$ is probably typical for the series, whereas in $(ET)_2ClO_4(TCE)_{0.5}$ one finds $\rho_\perp/\rho_{||} \simeq 1$–$2$ (*86*), which suggests a very two-dimensional electronic structure in agreement with other experimental results, as well as band structure calculations (*89*).

### 2. *Discussion*

The anistropy of a quasi-one-dimensional conductor provides considerable insight into the directional dependence of the electronic structure of the compound. It is, however, difficult to measure in $(TMTSF)_2X$ salts and in some of the (ET):X salts. Because of the low crystallographic symmetry, crystal faces are not perpendicular to high-symmetry directions. Nevertheless, adopting a simple tight-binding form for the electronic energy band:

$$\varepsilon(k) = 2t_a \cos(k_a a) + 2t_{b'} \cos(k_{b'} b') + 2t_{c^*} \cos[k_{c^*}(2\pi/c^*)],$$

with

$$k = k_a \hat{a} + k_{b'} \hat{b}' + k_{c^*} \hat{c}^*,$$

(where carets denote a unit vector) one may estimate the ratios between the transfer integrals $t_a, t_{b'}, t_{c^*}$ from the conductivity results. For a quasi-one-dimensional conductor, a rough estimate (*90*) for $\rho_{||}/\rho_\perp \simeq (t_\perp/t_{||})^2$, the anisotropy given above for $(TMTSF)_2PF_6$, yields $t_a:t_{b'}:t_{c^*} \simeq 1:\frac{1}{10}:\frac{1}{200}$, which is in rough agreement with more accurate determinations. In $(ET)_2ClO_4(TCE)_{0.5}$ the low anisotropy of the conductivity suggests a rather two-dimensional electronic structure in accordance with the crystallographic structure and the associated "corrugated sheet network" of *inter*stack S···S interactions (*56*).

## C. Pressure Studies

Because of the "softness" of organic metals one expects them to show interesting behavior under applied pressures. This had been demonstrated earlier by Jerome and co-workers on several compounds and in the case of TMTSF-DMTCNQ (DMTCNQ = dimethyltetracyanoquinodimethane) a pressure of 10 kbar transforms it abruptly from a Peierls semiconductor with $T_{MI} = 50$ K to a metal at all temperatures (*91*). When the temperature-dependent resistance of the $(TMTSF)_2X$ family became known, the very low transition temperatures in some of the compounds suggested that these salts would easily become metallic, and maybe even superconducting, under pressure.

### *1.* $(TMTSF)_2X$

Indeed the pressure dependence of the resistivity of $(TMTSF)_2X$ salts shows a very rich behavior. $(TMTSF)_2PF_6$ was the first organic metal to show superconductivity at a pressure of 6.5 kbar at 0.9 K (*7*). Up to this pressure the metal–insulator transition temperature gradually decreases, possibly with a strong dependence close to $P_c$. The superconducting transition temperature also decreases, but slowly, with increasing pressure. Several of the octahedral anion salts show the same behavior with somewhat different $P_c$ values, as one would expect from the anion volumes discussed above ($P_c$ values are listed in Table VI). The octahedral anion salts ($X = ReO_4^-$, $ClO_4^-$) show a greater variation in behavior than their tetrahedral counterparts, viz. $(TMTSF)_2ReO_4$ with $T_{MI} = 182$ K at ambient pressure and which becomes superconducting at 1.0 K above $P_c \simeq 12$ kbar, whereas $(TMTSF)_2ClO_4$ becomes superconducting at 1.2 K at ambient pressure (*70*). Both of these results are exciting and astonishing. First, the success with the $ClO_4^-$ salt may be considered the victory of more than two decades of struggle to find an organic superconductor; but, secondly, the $ReO_4^-$ salt demonstrated that superconductivity can be achieved with modest pressures even if the metal–insulator transition temperature is quite high.

The common pressure dependence of the $(TMTSF)_2X$ salts is illustrated in Fig. 20. Below the critical pressure $P_c$ the electronic ground state is an insulator of either the spin density wave type or the anion-assisted Peierls type. Above $P_c$ the ground state is superconducting. The critical pressure $P_c$ varies monotonically with the anion volume discussed above; but the transition temperature at ambient pressure and the type of low-pressure ground state depend specifically on the

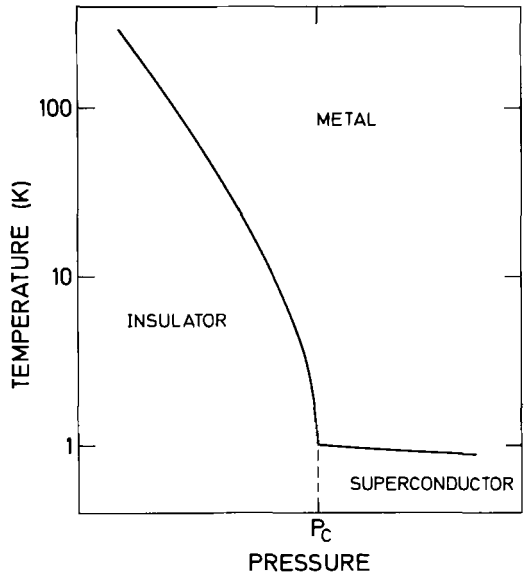


FIG. 20. Illustration of the temperature–pressure phase diagram for $(TMTSF)_2X$ salts. The critical pressure $P_c$ varies between ambient pressure and 12 kbar for different compounds.

symmetry of the anion. The latter observation demonstrates a correspondence between the lattice superstructure and the nature of the ground state, and this is substantiated by studies in $(TMTSF)_2ClO_4$ where the anion order can be obstructed by rapid cooling through $T_0 = 24$ K (*78, 92*). In this "quenched" state the salt has a spin density wave ground state associated with the "freezing in" of a $ClO_4^-$ anion disorder.

Since the ambient-pressure superconductor $(TMTSF)_2ClO_4$ has a very small anion volume, it is tempting to go to even smaller anions in order to increase the superconducting transition temperature. The cases $X = NO_3^-$, $BF_4^-$, and $H_2F_3^-$ are examples of such conductors but the existence of superconductivity has not been established in $(TMTSF)_2X$ salts for these anions. Lack of superconductivity suggests a different Se network in compounds with very small anions, and low-temperature structural results provide some evidence for this.

An unusual pressure-dependent resistivity has been reported for $(TMTSF)_2PO_2F_2$ (*47*). This compound has a metal–insulator transition at 135 K at ambient pressure, which is quite high considering that the anion volume of $PO_2F_2^-$ is very close to that of $ClO_4$. Furthermore, pressure has a relatively small effect, and even at pressures of 14.5 kbar

there is some indication of the transition. However, a crystallographic study performed at a temperature below $T_{MI}$ revealed a frozen-in $PO_2F_2^-$ anion disorder which is likely the cause of the transition (*48*).

*2.* $(ET)_2X$

Only in the case of the 2:1 $ReO_4^-$ salt, and of course $X = I_3^-$ and $IBr_2^-$, do the *properties* of the $(ET)_2X$ salts resemble the $(TMTSF)_2X$ series (*8*). With a critical pressure of 4–6 kbar, the $ReO_4^-$ salt fits the phase diagram in Fig. 20. The great similarity in properties of salts based on different molecules suggests that the solid-state environment is as crucial to the physical behavior as are the molecular characteristics.

## V. Magnetic Properties

The magnetic susceptibility $\chi(T)$ of organic conductors is of interest because it, in several ways, reflects properties other than the conductivity. In particular, it provides a clear means of discriminating between the CDW and the SDW states which conductivity measurements cannot distinguish. The value of $\chi$ may be measured by either static or resonance techniques. Static measurements contain in general contributions from (i) molecular core diamagnetism, (ii) Curie-like susceptibility stemming from localized spin-carrying defects, and (iii) spin susceptibility from the conduction electrons. Electron spin resonance (ESR) measures only the two latter contributions which contain the interesting information about the electronic properties of the conductor. In order to compare results of static and ESR measurements the temperature-independent contribution (i) must, therefore, be subtracted from the former. Furthermore, the ESR signal has a width which measures the interactions of the spins.

### A. Magnetic Susceptibility

*1.* $(TMTSF)_2X$

The room-temperature electronic susceptibility is typically $3 \times 10^{-4}$ emu $cm^3$ $mol^{-1}$ for $(TMTSF)_2X$ compounds and decreases approximately linearly with decreasing temperature until the transition occurs (*93–95*). Below the transition there is a clear distinction between the three possible ground states discussed above (*61, 94*). This

is illustrated in Fig. 21. In the case of an anion-assisted charge density wave system with $X = ReO_4^-$, $\chi$ becomes activated with an activation energy similar to $\Delta$ from conductivity, both when measured statically and by ESR (*95*). For spin density wave systems, e.g., $X = PF_6^-$, the situation is much more complicated (*94, 96*). Whereas the ESR signal vanishes both from decreasing $\chi$ as well as from line broadening, the static susceptibility vanishes only when the magnetic field is in the direction of the spins. Consequently $\chi$ has a strong directional dependence and in a powder, which is most often used in static measurements, only a very small anomaly is seen at $T_{MI}$. For superconducting

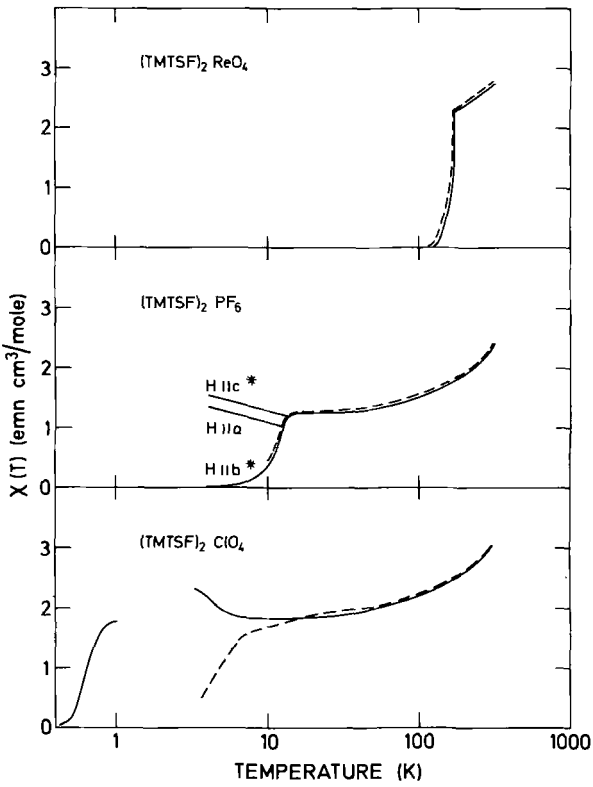


FIG. 21. Magnetic susceptibility of $(TMTSF)_2X$ salts with $X = ReO_4^-$, $PF_6^-$, and $ClO_4^-$. Full lines indicate static measurements on powders ($ReO_4^-$ and $ClO_4^-$) and on single crystals ($PF_6^-$). Dashed lines show ESR single-crystal results. The three cases illustrate anion-assisted charge density wave ($ReO_4^-$), spin density wave ($PF_6^-$), and spin density wave precursors of superconductivity ($ClO_4^-$). A separate result showing the superconducting transition is also shown for $X = ClO_4^-$.

$(TMTSF)_2ClO_4$ the two susceptibilities give evidence for an incomplete spin density wave transition at $T \simeq 5$ K at intermediate cooling rates reminiscent of the features in some conductivity measurements (*93*). At the superconducting transition the susceptibility vanishes, but the transition temperature is lower than that deduced from conductivity (*97*).

### 2. (ET):$ReO_4$

ESR measurements have been performed on three (ET): $ReO_4$ phases (*97*), but $\chi(T)$ is not known on an absolute scale. The results are shown in Fig. 22. The 2:1 salt has features similar to $(TMTSF)_2ReO_4$; it has a constant susceptibility in the metallic regime and an abrupt transition to a very low value below $T_{MI}$. The 3:2 salt has a $\chi(T)$ similar to what one expects from a Peierls transition without influence of anion ordering, i.e., somewhat similar to TTF-TCNQ if scaled to the present $T_{MI}$. Finally, the $2{:}1{:}\frac{1}{2}$ salt has a rather featureless susceptibility with a

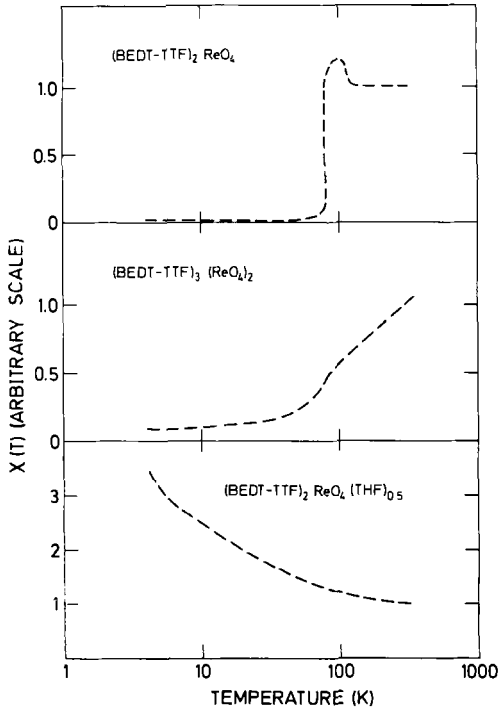


FIG. 22. The magnetic susceptibility of various ET:$ReO_4^-$ phases on an arbitrary scale.

Curie-like ($1/T$) tail at low temperatures, signifying a high concentration of defects.

### 3. *Discussion*

The high-temperature susceptibility may be understood as originating from two contributions. First, the so-called Pauli susceptibility stems from the band nature of the electronic states. It may be calculated from the transfer integral $t_{||}$, which from optical measurements and calculations is 260 meV for $(TMTSF)_2X$ salts and corresponds to a bandwidth of 1.1 eV. The contribution to $\chi(T)$ is a temperature-independent susceptibility of $0.6 \times 10^{-4}$ emu cm$^3$ mol$^{-1}$, approximately half the measured $\chi$ at temperatures just above $T_{MI}$. This excess susceptibility is attributed to a "correlation enhancement" owing to the Coulombic repulsion between electrons. This effect is often parameterized into an on-site Coulombic energy, the "Hubbard $U$." An enhancement factor of 2 as observed for $(TMTSF)_2X$ gives $U = 4t_{||}$ according to the zero-temperature theory of Takahashi (*98*), but later analysis with the temperature dependence of $\chi$ taken into account yields $U/4t_{||} = 0.4$ (*99*). These values for $U/4t_{||}$ are typical of good organic conductors but the importance of correlations is difficult to assess from such estimates of $U/4t_{||}$. However, it should be noted that there is no evidence for strong effects on the conductivity originating from the dimerization gap in the electronic band structure, so in this respect $U$ is not large in $(TMTSF)_2X$ salts.

The low value of $U$ in $(TMTSF)_2X$ salts in view of their $\frac{3}{4}$ filled electron band (or the $\frac{1}{4}$ hole band) is in striking contrast to the high $U$s in $\frac{1}{4}$-filled $M(TCNQ)_2$ conductors, which often have a susceptibility enhancement over the Pauli susceptibility of factors of 10–30, suggesting that $U/4t_{||} \gg 1$. As pointed out by Mazumdar and Bloch (*100*), $U$ is an effective parameter which is "magnified" at the band filling of $\frac{1}{4}$. This makes it much easier to understand why $M(TCNQ)_2$ and $(TMTTF)_2X$ salts show strong correlation effects and why in $(TMTSF)_2X$ salts $U$ is so low.

With respect to the $(ET):ReO_4$ salts, a similar analysis cannot be carried out since the absolute value of $\chi$ is not known. However, the fact that $\chi(T)$ is constant above $T_{MI}$ in the 2:1 salts suggests a low value of $U/4t_{||}$.

The low-temperature behavior of $\chi(T)$ can be understood from the usual concepts of a charge density wave, where the abruptness of the phase transition seems to be the major signature of the effects of anion ordering on the magnetic properties. In the case of the spin density wave, Overhauser's theory for itinerant antiferromagnetism gives a

satisfactory description of the observed phenomena (*101*). Regarding the superconducting transition temperature in $(TMTSF)_2ClO_4$, which is lower when measured by susceptibility than by conductivity, a possible explanation is as follows. At some temperature superconducting lamellae develop, presumably parallel to *ab* planes, giving a zero resistance; but in between the lamellae, the normal metal still contributes to $\chi(T)$. Only when the entire crystal at some lower temperature is in its zero-resistance state does one observe the magnetic transition.

## B. ESR Linewidths

In Fig. 23 we show the ESR linewidths $\Delta H_{pp}$ for the six compounds discussed above. The larger widths of $(TMTSF)_2X$ salts, compared to the (ET):$ReO_4$ derivatives, is due to the larger spin–orbit coupling in Se than in S. Apart from this, the linewidths show the following features.

1. In the case of an anion-assisted Peierls transition, the linewidth changes abruptly, e.g., $(TMTSF)_2ReO_4$ and $(ET)_2ReO_4$, whereas the usual Peierls transition in $(ET)_3(ReO_4)_2$ is more gradual.
2. The linewidth increases below a spin density wave transition.

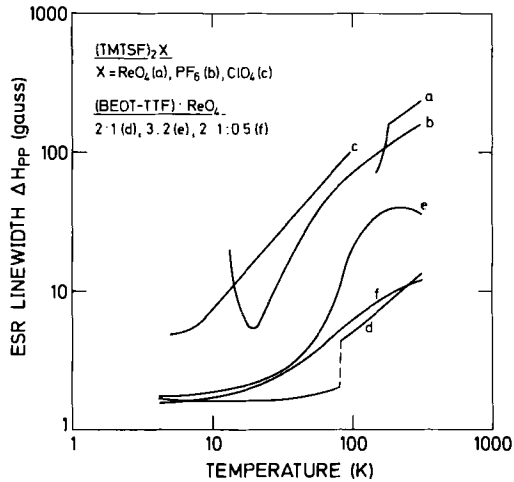


FIG. 23. A comparison of the ESR linewidths of various $(TMTSF)_2X$, X = monovalent anion, and ET:$ReO_4^-$ salts.

3. Even in the absence of a transition, the linewidth does change appreciably with temperature. Hence, the ESR lineshape $\Delta H_{pp}$ provides a good means of discriminating between the different phases of the salt (*83, 97*). For example, ΔHpp (298 K) is ~20 gauss in $\beta$-$(ET)_2I_3$ and 95 gauss in $\alpha$-$(ET)_2I_3$ (*83*).

## VI. Concluding Remarks

From structural and transport studies of the organic conductors based on $(TMTSF)_2X$ and $(ET)_2X$, their varied properties appear both rich and complex. Although charmed by their unique richness, but often frustrated by their complexity, we are, nevertheless, able to point out several cases of correspondence between their crystallographic and physical properties, which may be summarized as follows.

1. As synthetic metals they are by no means unique in terms of high metallic conductivity since several salts of other systems have higher conductivity. This is in agreement with both experimental and theoretical results based on their intrachain electronic bandwidth $4t_{||}$, which is not particularly high, and certainly very small compared to ordinary metals.
2. A unique feature is, however, the very small role that Coulomb interactions play, in particular when considering their stoichiometry. Their low values of $U$ are, at least in part, a molecular property, but studies of different phases of $ET:ReO_4$ indicate that $U$ depends specifically upon the crystallographic environment. That the electrons are not strongly influenced by Coulomb repulsions appears to be necessary for superconductivity.
3. As one-dimensional conductors, they are often not very one-dimensional. Both from a crystallographic as well as from an electronic point of view these compounds have a rather strong coupling between the stacks. There is variation in this coupling within both the $(TMTSF)_2X$ and the (ET):X series, although the variation is much greater in the latter case. It is likely that the richness in behavior is related to a crossover in effective dimensionability, from compound to compound, or as a function of pressure in one compound, so that both one-dimensional instabilities (spin density and charge density waves) as well as three-dimensional superconductivity may occur.

For the isostructural series $(TMTSF)_2X$ the differences in physical behavior for different anions X are associated with very minute changes in the crystallographic structure. The anion volume

determines uniquely the unit cell volume, but in particular, the average *inter*stack Se···Se distance, which is directly related to the dimensionality, and this seems to correlate with the occurrence of superconductivity. The symmetry of the anion also plays a determining role as it is responsible for structural order–disorder transitions of varying symmetries. In the case of the Peierls transition there is a direct relation between the symmetry (or periodicity) of this superlattice and the symmetry of the Peierls instability, but the role of symmetry is not understood in detail. The same is true for the role of disorder since superconductivity is not destroyed by disorder in ordinary superconductors, whereas in $(TMTSF)_2X$ organic superconductors it appears to be. A possible explanation for this could be that ordering influences the interchain distances enough to change the effective dimensionality.

It is clear that the field of organic conductors is continually providing new and unusual materials for study by chemists, physicists, materials scientists, and theorists. There is no doubt that the potential for future surprises in this area of research is bright.

ACKNOWLEDGMENTS

J.M.W. wishes to acknowledge the invaluable collaboration of the colleagues and students whose names appear in many of the articles cited, and he expresses his special thanks to Drs. M. A. Beno, P. C. W. Leung, T. J. Emge, H. H. Wang, A. J. Schultz, and Mrs. V. Bowman for her excellent editorial assistance on this manuscript. Similarly, K.C. would like to thank K. Bechgaard, C. S. Jacobsen, and J. C. Scott.

This study was supported in part by NATO (Grant No. 016.81). We also want to thank our laboratories for the mutual hospitality and support extended to us during visits abroad. Work at Argonne National Laboratory is sponsored by the United States Department of Energy, Office of Basic Energy Sciences, Division of Materials Science, under Contract W-31-109-ENG-38.

REFERENCES

1. Akamatu, H., Inokuchi, H., and Matsunaga, Y., *Nature (London)* **173,** 168 (1954).
2. Acker, D. S., Harder, R. J., Hertler, W. R., Mahler, W., Melby, L. R., Benson, R. E., and Mochel, W. E., *J. Am. Chem. Soc.* **82,** 6408 (1960).
3. Bardeen, J., Cooper, L. N., and Schrieffer, J. R., *Phys. Rev.* **108,** 1175 (1957).
4. Little, W. A., *Phys. Rev. A* **134,** 1416 (1964).
5. Coleman, L. B., Cohen, M. J., Sandman, D. J., Yamagishi, F. G., Garito, A. F., and Heeger, A. J., *Solid State Commun.* **12,** 1125 (1973).
6. Peierls, R. E., "Quantum Theory of Solids," p. 107. Oxford Univ. Press, London and New York, 1954.
7. Jerome, D., Mazaud, A., Ribault, M., and Bechgaard, K., *J. Phys. Lett.* **41,** 95 (1980).
8. Parkin, S. S. P., Engler, E. M., Schumaker, R. R., Lagier, R., Lee, V. Y., Scott, J. C., and Greene, R. L., *Phys. Rev. Lett.* **50,** 270 (1983).
9. Yagubskii, E. B., Shchegolev I. F., Laukhin, V. N., Kononovich, P. A., Karatsovnik, M. W., Zvarykina A. V., and Buravov, L. I., *JETP Lett. (Engl. Trans.)* **39,** 12 (1984).
10. Bechgaard, K., *Mol. Cryst. Liq. Cryst.* **79,** 1 (1981).
11. Bechgaard, K., Carneiro, K., Rasmussen, F. B., Olsen, M., Rindorf, G., Jacobsen, C. S., Pedersen, H., and Scott, J. C., *J. Am. Chem. Soc.* **103,** 2440 (1981). [There is an

error in footnote 10; $(TMTSF)_2ClO_4$ was prepared by anodic oxidation of $10^{-3}$ *M* (not $10^{-5}$ *M*) (TMTSF)].

12. Jacobsen, C. S., Williams, J. M., and Wang, H. H., *Solid State Commun.* **54,** 937 (1985).
13. Bechgaard, K., Cowan, D. O., and Bloch, A. N., *J. Chem. Soc., Chem. Commun.*, p. 937 (1974).
14. Andersen, J. R., and Bechgaard, K., *J. Org. Chem.* **40,** 2016 (1975).
15. Bechgaard, K., Cowan, D. O., Bloch, A. N., and Henriksen, L., *J. Org. Chem.* **40,** 746 (1975).
16. Cowan, D. O., Bloch, A. N., and Bechgaard, K., U. S. Pat. 4,246,173 (1981).
17. Shu, P., Bloch, A. N., Carruthers, T. F., and Cowan, D. O., *J. Chem. Soc., Chem. Commun.*, p. 505 (1977).
18. Wudl, F., and Nalewajek, D., *J. Chem. Soc., Chem. Commun.*, p. 866 (1980).
19. Wudl, F., Aharon-Shalom, E., and Bertz, S. H., *J. Org. Chem.* **46,** 4612 (1981).
20. Braam, J. M., Carlson, C. D., Stephens, D. A., Rehan, A. E., Compton, S. J., and Williams, J. M., *Inorg. Synth.* **24** (1985).
21. Spector, W. S., ed., "Handbook of Toxicology," Vol. I, p. 340. Saunders, Philadelphia, 1956.
22. Moradpour, A., Peyrussan, V., Johansen, I., and Bechgaard, K., *J. Org. Chem.* **48,** 388 (1982).
23. Moradpour, A., Bechgaard, K., Barrie, M., Lenoir, C., Murata, K., Lacoe, R. C., Ribault, M., and Jerome, D., *Mol. Cryst. Liq. Cryst.* **119,** 69 (1985).
24. Engler, E. M., and Patel, V. V., *J. Am. Chem. Soc.* **96,** 7376 (1974).
25. Lerstrup, K., Lee, M., Wiygul, F. M., Kistenmacher, T. J., and Cowan, D. O., *J. Chem. Soc., Chem. Commun.*, p. 294 (1983).
26. Johannsen, I., Bechgaard, K., Mortensen, K., and Jacobsen, C. S., *J. Chem. Soc., Chem. Commun.*, p. 295 (1983).
27. Mizuno, M., Garito, A. F., and Cava, M. P., *J. Chem. Soc., Chem. Commun.*, p. 18 (1978).
28. Reed, P. E., Braam, J. M., Sowa, L. M., Barkhau, R. A., Blackman, G. S., Cox, D. D., Ball, G. A., Wang, H. H., and Williams, J. M., submitted for publication.
29. Krug, W. P., Ph.D. Dissertation, Johns Hopkins University, Baltimore, Maryland (1977).
30. Schumaker, R. R., Lee, V. Y., and Engler, E. M., *J. Phys., Colloq.* **44,** C3-1139 (1983).
31. Saito, G., Enoki, T., Toriumi, T., and Inokuchi, H., *Solid State Commun.* **42,** 557 (1982).
32. Williams, J. M., Beno, M. A., Appelman, E. H., Capriotti, J. M., Wudl, F., Aharon-Shalom, E., and Nalewajek, D., *Mol. Cryst. Liq. Cryst.* **79,** 319 (1982).
33. Thorup, N., Rindorf, G., Soling, H., and Bechgaard, K., *Acta Crystallogr., Sect. B* **37,** 1236 (1981).
34. Soling, H., Rindorf, G., and Thorup, N., *Cryst. Struct. Commun.* **11,** 1980 (1982).
35. Tanaka, C., Tanaka, J., Dietz, K., Katayama, C., and Tanaka, M., *Bull. Chem. Soc. Jpn.* **56,** 405 (1983).
36. Soling, H., Rindorf, G., and Thorup, N., *Acta Crystallogr. Sect. C: Cryst. Struct. Commun.* **39,** 490 (1983).
37. Rindorf, G., Soling, H., and Thorup, N., *Acta Crystallogr., Sect. B* **38,** 2805 (1982).
38. Guy, D. R. P., Boebinger, G. S., Marseglia, E. A., and Friend, R. H., *J. Phys. C* **16,** 691 (1983).
39. Williams, J. M., Beno, M. A., Banovetz, L. M., Braam, J. M., Blackman, G. S., Carlson, C. D., Greer, D. L., Loesing, D. M., and Carneiro, K., *J. Phys. Colloq.* **44,** C3-941 (1983).
40. Williams, J. M., Beno, M. A., Sullivan, J. C., Banovetz, L. M., Braam, J. M., Blackman, G. S., Carlson, C. D., Greer, D. L., and Loesing, D. M., *J. Am. Chem. Soc.* **105,** 643 (1983).

41. Kistenmacher, T. J., Emge, T. J., Shu, P., and Cowan, D. O., *Acta Crystallogr., Sect. B* **35,** 772 (1979).
42. Whangbo, M. H., Williams, J. M., Beno, M. A., and Dorfman, J. R., *J. Am. Chem. Soc.* **105,** 645 (1983).
43. Huheey J. E., "Inorganic Chemistry—Principles of Structure and Reactivity," 2nd Ed., p. 71. Harper, New York, 1978.
44. Shannon R. D., and Prewitt, C. T., *Acta Crystallogr., Sect. B* **25,** 925 (1969); Shannon, R. D., *Acta Crystallogr., Sect. A* **32,** 751 (1976).
45. Teramae, H., Tanaka, K., Shiotani, K., and Yamabe, T., *Solid State Commun.* **46,** 633 (1983).
46. Teramae, H., Tanaka, K., and Yamabe, T., *Solid State Commun.* **44,** 431 (1982).
47. Cox, S., Boysel, R. M., Moses, D., Wudl, F., Chen, J., Ochsenbein, S., Heeger, A. J., Walsh, W. M., Jr., and Rupp, L. W., *Solid State Commun.* **49,** 259 (1984).
48. Eriks, W., Wang, H. H., Reed, P. E., Beno, M. A., Appelman, E. H., and Williams, J. M., *Acta Crystallogr., Sect. C: Cryst. Struct. Commun.* **41,** 257 (1985).
49. Morosin, B., Schirber, J. E., Greene, R. L., and Engler, E. M., *Phys. Rev. B: Condens. Matter* **26,** 2660 (1982).
50. Williams, J. M., Beno, M. A., Sullivan, J. C., Banovetz, L. M., Braam, J. M., Blackman, G. S., Carlson, C. D., Greer, D. L., Loesing, D. M., and Carneiro, K., Phys. Rev. *B: Condens. Matter* **28,** 2873 (1983).
51. Thorup, N., Rindorf, G., Soling, H., Johannsen, I., Mortensen, K., and Bechgaard, K., *J. Phys. Colloq.* **44,** C3-1017 (1983).
52. Pauling, L., "The Nature of the Chemical Bond," 3rd ed., pp. 537–540. Cornell Univ. Press, Ithaca, New York, 1960.
53. Beno, M. A., Blackman, G. S., Leung, P. C. W., and Williams, J. M., *Solid State Commun.* **48,** 99 (1983).
54. Pouget, J. P., Shirane, G., Bechgaard, K., and Fabre, J. M., *Phys. Rev. B: Condens. Matter* **27,** 5203 (1983).
55. Emery, V. J., Bruinsma, R., and Barisic, S., *Phys. Rev. Lett.* **48,** 1039 (1982).
56. Williams, J. M., Beno, M. A., Wang, H. H., Reed, P. E., Azevedo, L. J., and Schirber, J. E., *Inorg. Chem.* **23,** 1790 (1984).
57. Parkin, S. S. P., Engler, E. M., Schumaker, R. R., Lagier, R., Lee, V. Y., Voiron, J., Carneiro, K., Scott, J. C., and Greene, R. L., *J. Phys. Colloq.* **44,** C3-791 (1983).
58. Kaminskii, V. F., Prokhorova, T. G., Shibaeva, R. P., and Yagubskii, E. B., *JETP Lett. (Engl. Transl.)* **39,** 17 (1984).
59. Kobayashi, H., Kobayashi, A., Sasaki, Y., Saito, G., Enoki T., and Inokuchi, H., *J. Am. Chem. Soc.* **105,** 297 (1983).
60. Kobayashi, H., Mori, T., Kato, R., Kobayashi, A., Sasaki, Y., Saito, G., and Inokuchi, H., *Chem. Lett.*, p. 681 (1983).
61. Bychkov, Y. A., Gor'kov, L. P., and Dzyaloshinskii, I. E., *Sov. Phys. JETP (Engl. Transl.)* **23,** 489 (1966); for reviews see Emery, V. J., *in* "Highly Conducting One-Dimensional Solids" (J. T. Devreese, R. P. Evrard, and V. E. Van Doren, eds.), p. 247. Plenum, New York, 1979; Solyom, J., *Adv. Phys.* **28,** 201 (1979).
62. Williams, J. M., Schultz, A. J., Underhill, A. E., and Carneiro, K., *in* "Extended Linear Chain Compounds" (J. S. Miller, ed.), Vol. I, p. 73. Plenum, New York, 1982; also see Williams, J. M., *Adv. Inorg. Chem. Radiochem.* **26,** 235 (1983).
63. Kohn, W., *Phys. Rev. Lett.* **2,** 393 (1959).
64. For reviews and background on X-ray diffuse and inelastic neutron scattering studies see Comès, R., *in* "One Dimensional Conductors" (H. G. Schuster, ed.), p. 32. Springer-Verlag, Berlin and New York, 1975; Renker, B., Pintschovius, P. Glaeser, W. Rietschel, H., and Comès, R., *ibid,* p. 53; Renker, B., and Comès, R., *in* "Low Dimensional Coorperative Phenomena" (J. H. Keller, ed.), p. 235. Plenum, New York,

1975; Megtert, S., Pouget, J. P., and Comès, R., *Ann. N. Y. Acad. Sci.* **313,** 234 (1973).
65. Mortensen, K., Jacobsen, C. S., Lindegaard-Andersen, A., and Bechgaard, K., *J. Phys. Colloq.* **44,** C3-963 (1983).
66. Pouget, J. P., Moret, R., Comès, R., Bechgaard, K., Fabre, J. M., and Giral, L., *Mol. Cryst, Liq. Cryst.* **79,** 129 (1982).
67. Torrance, J. B., Pedersen, H. J., and Bechgaard, K., *Phys. Rev. Lett.* **49,** 881 (1982), and references therein.
68. Williams, J. M., in preparation.
69. Moret, R., Pouget, J. P., Comès, R., and Bechgaard, K., *J. Phys. Colloq.* **44,** C3-957 (1983), and references therein.
70. Gubser, D. U., Fuller, W. W., Poehler, T. O., Stokes, J., Cowan, D. O., Lee, M., and Bloch, A. N., *Mol. Cryst. Liq. Cryst.* **79,** 225 (1982).
71. Pouget, J. P., Shirane, G., Bechgaard, K., and Fabre, J. M., *Phys. Rev. B: Condens. Matter* **27,** 5203 (1983).
72. Pouget, J. P., Moret, R., Comès, R., Shirane, G., Bechgaard, K., and Fabre, J. M., *J. Phys. Colloq.* **44,** C3-969 (1983).
73. Tomíc, S., Pouget, J. P., Jerome, D., Bechgaard, K., and Williams J. M., *J. Phys. (Paris)* **44,** 375 (1983).
74. Pouget, J. P., Moret, R., Comès, R., and Bechgaard, K., *J. Phys. Lett.* **42,** 543 (1981).
75. Jacobsen, C. S., Pedersen, H. J., Mortensen, K., Rindorf, G., Thorup, N., Torrance, J. B., and Bechgaard, K., *J. Phys. C* **15,** 2651 (1982).
76. Moret, R., Pouget, J. P., Comès, R., and Bechgaard, K., *Phys. Rev. Lett.* **49,** 1008 (1982).
77. Wudl, F., Aharon-Shalom, E., Nalewajek, D., Waszczak, J. V., Walsh, W. M., Jr., L. W., Rupp, Jr., Chaikin, P., Lacoe, R., Burns, M., Poehler, T. O., Beno, M. A., and Williams, J. M., *J. Chem. Phys.* **76,** 5497 (1982).
78. Takahashi, T., Jérome, D. D., and Bechgaard, K., *J. Phys. Lett.* **43,** 565 (1982).
79. Fournel, A., More, C., Roger, G., Sorbier, J. P., Delrieu, J. M., Jerome, D., Ribault, M., and Bechgaard, K., *J. Phys. Lett.* **42,** 445 (1981).
80. Kagoshima, S., Pouget, J. P., Saito, G., and Inokuchi, H., *Solid State Commun.* **45,** 1001 (1983).
81. Bechgaard, K., Jacobsen, C. S., Mortensen, K., Pedersen, H. J., and Thorup, N., *Solid State Commun.* **33,** 1119 (1980).
82. Bechgaard, K., Jacobsen, C. S., and Hessel Andersen, N., *Solid State Commun.* **25,** 875 (1978).
83. Leung, P. C. W., Beno, M. A., Emge, T. J., Wang, H. H., Bowman, M. K., Firestone, M. A., Sowa, L. M., and Williams, J. M., *Mol. Cryst. Liq. Cryst.* **125,** 113 (1985).
84. Maaroufi, A., Coulon, C., Flandrois, S., Delhaes, P., Mortensen, K., and Bechgaard, K., *Solid State Commun.* **48,** 555 (1983).
85. Mortensen, K., Jacobsen, C. S., Bechgaard, K., and Williams, J. M., *Synth. Met.* **9,** 63 (1984).
86. Friend, R. H., Jérome, D., Fabre, J. M., Giral, L., and Bechgaard, K., *J. Phys. C* **11,** 263 (1978).
87. Kobayashi, H., Kato, R., Mori, T., Kobayashi, A., Sasaki, Y., Saito, G., and Inokuchi, H., *Chem. Lett.*, p. 759 (1983).
88. Jacobsen, C. S., Mortensen, K., Thorup, N., Tanner, D. B., Weger, M., and Bechgaard, K., *Chem. Scr.* **17,** 103 (1981).
89. Mori, T., Kobayashi, A., Sasaki, Y., Kobayashi, H., Saito, G., and Inokuchi, H., *Chem. Lett.*, p. 1963 (1982).
90. Soda, G., Jérome, D., Weger, M., Alizon, J., Gallice, J., Robert, H., Fabre, J. M., and Giral, L., *J. Phys. (Paris)* **38,** 931 (1977).
91. Andrieux, A., Duroure, C., Jerome D., and Bechgaard, K., *J. Phys. Lett.* **40,** 381 (1979).
92. Garoche, P., Brusetti, R., and Bechgaard, K., *Phys. Rev. Lett.* **49,** 1346 (1982).

*93.* Scott, J. C., *Mol. Cryst. Liq. Cryst.* **79,** 49 (1982).
*94.* Scott, J. C., Pedersen, H. J., and Bechgaard, K., *Phys. Rev. B: Condens. Matter* **24,** 475 and 5014 (1981).
*95.* Pedersen, H. J., Scott, J. C., and Bechgaard, K., *Phys. Scr.* **25,** 849 (1982).
*96.* Mortensen, K., Tomkiewicz, Y., and Bechgaard, K., *Phys. Rev. B: Condens. Matter* **25,** 3319 (1982).
*97.* Carneiro, K., Scott, J. C., and Engler, E. M., *Solid State Commun.* **50,** 477 (1984).
*98.* Takahashi, M., *Prog. Theor. Phys.* **40,** 348 (1970).
*99.* Tanaka, J., and Tanaka, C., *J. Phys. Colloq.* **44,** C3-997 (1983).
*100.* Mazumdar, S., and Bloch, A. N., *Phys. Rev. Lett.* **50,** 207 (1983).
*101.* Overhauser, A. W., *Phys. Rev.* **128,** 1437 (1962).
*102.* Mori, T., Kobayashi, A., Sasaki, Y., Kobayashi, H., Saito, G., and Inokuchi, H., *Chem. Lett.*, p. 957 (1984).
*103.* Leung, P. C. W., Beno, M. A., Blackman, G. S., Coughlin, B. R., Miderski, C. A., Joss, W., Crabtree, G. W., and Williams, J. M., *Acta Crystallogr. Sect. C: Cryst. Struct. Commun.* **40,** 1331 (1984).
*104.* Parkin, S. S. P., Creuzet, F., Ribault, M., Jerome, D., Bechgaard, K., and Fabre, J. M., *Mol. Cryst. Liq. Cryst.* **79,** 249 (1981).
*105.* Crabtree, G. W., Carlson, K. D., Hall, L. N., Copps, P. T., Wang, H. H., Emge, T. J., Beno, M. A., and Williams, J. M., *Phys. Rev. B: Condens. Matter* **30,** 2958 (1984).
*106.* Williams, J. M., Emge, T. J., Wang, H. H., Beno, M. A., Copps, P. T., Hall, L. N., Carlson, K. D., and Crabtree, G. W., *Inorg. Chem.* **23,** 2558 (1984).
*107.* Carlson, K. D., Crabtree, G. W., Hall, L. N., Behroozi, F., Copps, P. T., Sowa, L. M., Nuñez, L., Firestone, M. A., Wang, H. H., Beno, M. A., Emge, T. J., and Williams, J. M., *Mol. Cryst. Liq. Cryst.* **125,** 159 (1985).
*108.* Williams, J. M., Wang, H. H., Beno, M. A., Emge, T. J., Sowa, L. M., Copps, P. T., Behroozi, F., Hall, L. N., Carlson, K. D., and Crabtree, G. W., *Inorg. Chem.* **23,** 3839 (1984).
*109.* Kobaysahi, H., Kobayashi, A., Saito, G., Inokuchi, H., *Chem. Lett.*, p. 245 (1982).
*110.* Rindorf, G., Soling, H., and Thorup, N., *Acta Crystallogr. Sect. C: Cryst. Struct. Commun.* **40,** 1137 (1984).
*111.* Bender, K., Dietz, K., Endres, H., Helberg, H. W., Hennig, I., Keller, H. J., Schafer, H. W., and Schweitzer, D., *Mol. Cryst. Liq. Cryst.* **107,** 45 (1984).
*112.* Emge, T. J., Leung, P. C. W., Beno, M. A., Schultz, A. J., Wang, H. H., Sowa, L. M., and Williams, J. M., *Phys. Rev. B: Condens, Matter* **30,** 6780 (1984).
*113.* Leung, P. C. W., Emge, T. J., Beno, M. A., Wang, H. H., Williams, J. M., Petricek, V., and Coppens, P., *J. Am. Chem. Soc.* **106,** 7644 (1984); *Mol. Cryst. Liq. Cryst.* **119,** 347 (1985).
*114.* Carlson, K. D., Crabtree, G. W., Hall, L. N., Copps, P. T., Wang, H. H., Emge, T. J., Beno, M. A., and Williams, J. M., *Mol. Cryst. Liq. Cryst.* **119,** 357 (1985).
*115.* Yagubskii, E. B., Shchegolev, I. F., Pesotskii, S. I., Laukhin, V. N., Kononovich, P. A., Karatsovnik, M. V., and Zvarykina, A. V., *JETP Lett. (Engl. Transl.)* **39,** 328 (1984).
*116.* Shibaeva, R. P., Kaminskii, V. F., Yagubskii, E. B., *Mol. Cryst. Liq. Cryst.* **119,** 361 (1985).
*117.* Wang, H. H., Beno, M. A., Geiser, U., Firestone, M. A., Webb, K. S., Nuñez, L., Crabtree, G. W., Carlson, K. D., Williams, J. M., Azevedo, L. J., Kwah, J. F., and Schirber, J. E., *Inorg. Chem.* **24,** 2465 (1985).

NOTE ADDED IN PROOF. Since the preparation of the original manuscript, *ambient pressure* superconductivity has been reported in $\beta$-$(ET)_2AuI_2$ (*117*). The transition temperature ($T_c$ = 5 K) is the highest reported to date.